Renewable Energy 242 (2025) 122401

Contents lists available at ScienceDirect

Renewable Energy

journal homepage: www.elsevier.com/locate/renene

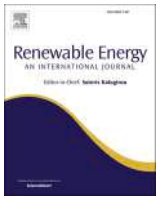

Reusing oil and gas exploration data to derisk geothermal projects: The Guardia Lombardi case study (Southern Italy)

Michele Livani [a,*], Barbara Inversi [b], Giordano Montegrossi [c,d], Lorenzo Petracchini [a], Claudio Alimonti [a,e], Davide Scrocca [a]

[a] CNR, Istituto di Geologia Ambientale e Geoingegneria, c/o Dipartimento di Scienze della Terra, Sapienza Università di Roma, P. le A. Moro 5, 00185, Roma, Italy
[b] Gartner Italia Srl, Via Caldera 21, 20153, Milano, Italy
[c] CNR, Istituto di Geoscienze e Georisorse, Via G. La Pira 4, 50121, Firenze, Italy
[d] INSTM, Consorzio Interuniversitario Nazionale per la Scienza e Tecnologia dei Materiali, Via G. Giusti 9, 50121, Firenze, Italy
[e] Sapienza Università di Roma, Dipartimento Ingegneria Chimica Materiali Ambiente (DICMA), Via Eudossiana 18, 00184, Roma, Italy

ARTICLE INFO

Keywords:
Geothermal energy
geothermal reservoir
green energy transition
3D geological modeling
Numerical modeling

ABSTRACT

Geothermal energy plays a key role in the green energy transition since it represents a low-carbon alternative to traditional fuels, but the high exploration costs and mining risks still hinder its use. Therefore, the reuse of pre-existing subsurface geological data can represent a way to counteract these limiting factors and promote the use of geothermal resources.

We reconstructed a 3D geological model of the Guardia Lombardi area (Campania Region, southern Italy) and evaluated its geothermal potential interpreting vintage oil and gas subsurface data (i.e., seismic reflection profiles and well data). The exploitation potential of the geothermal resource and the related costs were also evaluated.

The study revealed the presence of a geothermal reservoir with 125 °C at just 2300 m depth and an exploitation potential of about 70 kg/s, employable for residential heating and/or cooling and for electricity production in the nearby Grottaminarda town, with an appreciable economic benefit.

These results demonstrate how the reuse of pre-existing subsurface geological data provided by past oil & gas exploration can considerably reduce costs and mining risks associated with geothermal resource exploration, contributing to a faster and considerable reduction in CO_2 emissions.

1. Introduction

To date, the pressing necessity to reduce the greenhouse gas emissions and achieve the carbon neutrality by 2050 [1–3] against the global warming-related phenomena [4–9] requires the adoption of urgent countermeasures, first of all the green energy transition.

In this context, geothermal energy seems very promising [10] because it can significantly contribute to the diffusion of low-carbon technologies for electricity generation and building heating/cooling [11,12]. However, up to now, geothermal energy use was limited due to various factors, among which: i) the high costs of geothermal exploration for well drilling and data acquisition [11], and ii) the mining risks, primarily the exploration failure. As a matter of fact, almost all the world's major sedimentary basins have been explored for various purposes, especially for hydrocarbon exploration and production. These exploration activities have generated a huge amount of valuable subsurface data such as 2D and 3D seismic reflection data and detailed well information (e.g., reservoirs poro-perm properties, pressure, temperature, and geofluid composition), even in areas where no exploitable oil and gas (hereinafter O&G) fields were discovered. In the new context of energy system decarbonization and to contain data acquisition costs and mining risks, it becomes possible to take advantage of these pre-existing data for the exploration, characterization, and evaluation of the geothermal resource as already successfully done, for instance, in Germany [13] or in the Nederland [14].

Italy is one of the major geothermal energy producers in the world [15]. The potentially extractable and exploitable geothermal energy is estimated to be between 5800 and 116,000 TWh of energy, against an annual demand slightly above 300 TWh [16]. However, the geothermal resource exploitation in Italy is negligible compared to its potential; just under 2 percent of the national energy needs are produced from

* Corresponding author
E-mail address: michele.livani@cnr.it (M. Livani).

https://doi.org/10.1016/j.renene.2025.122401
Received 20 September 2024; Received in revised form 18 December 2024; Accepted 11 January 2025
Available online 13 January 2025

Abbreviations

AI	Artificial Intelligence
ARERA	Autorità di Regolazione per Energia Reti e Ambiente
BHT	Bottom-Hole Temperature
CAPEX	CApital EXpenditure
COP	COnference of the Parties
DH	Down Hole
DST	Drill Stem Test
EGEC	European Geothermal Energy Council
GLE	Ground Level Elevation
IRR	Internal Rate of Return
K eff	Effective permeability
LCCA	life cycle cost assessment
LCOH	Levelized COst of Heat
MD	Measured depth
NPV	Net Present Value
O&G	Oil and Gas
OPEX	OPerational EXpenditure
ORC	Organic Rankine Cycle
PBT	PayBack Time
Phi	Porosity
RTE	Rotary Table Elevation
SBHT	Static Bottom-Hole Temperature
TD	Total depth
TVDSSL:	True Vertical Depth Sub Sea Level
ViDEPI	Visibilità dei Dati afferenti all'attività di Esplorazione Petrolifera in Italia

geothermal energy source [15]. In addition to its great geothermal potential, Italy has an extensive history of hydrocarbon exploration, which has resulted in the availability of numerous geological and geophysical subsurface data.

In this contribution, we demonstrate how the assessment of the geothermal resources may take advantage of the previous O&G exploration activities focusing on a case study in Italy. Our case study is the Guardia Lombardi area (Campania Region, southern Italy; Fig. 1), which was intensively explored for hydrocarbon exploration purposes during the 1950s–1970s [17–19] making available a relevant amount of subsurface data, including seismic reflection profiles and well data [20,21] (Fig. 1). The Guardia Lombardi area has been analyzed within the framework of VIGOR project, aimed at the evaluation of the geothermal potential of Campania, Calabria, Puglia and Sicily regions, in southern Italy [22–24], while other subsequent numerical simulations of the reservoir behavior have confirmed the geothermal potential of this area [25,26].

The published and available geophysical, geothermal, geochemical and hydrogeological data provide several evidences of the presence of a subsurface thermal anomaly in the Guardia Lombardi area, such as: i) high heat flow up to 90 mW/m^2 (Fig. 1) [27]; ii) temperatures in deep wells higher than 100 °C [27–29] (Fig. 1); iii) presence of thermal springs with temperature of about 27°–29 °C (e.g., the San Teodoro hypothermal spring Fig. 1) [30]; iv) Springs with high CO_2 concentration in water (e.g., Mefitiniella) and natural emission of low temperature CO_2 rich gasses (e.g., Mefite d'Ansanto with a total gas flux 23.1 kg/s; Fig. 1) [31–34]; v) geothermal reservoir temperature of 124 °C based on geothermometers on water samples collected from thermal springs [35].

The critical analysis of the available wealth of data allowed an accurate 3D definition of the geothermal reservoir and the development of numerical simulations of the reservoir behavior that demonstrated the feasibility of the exploitation of the geothermal resources in the Guardia Lombardi area. Finally, a possible use of the detected geothermal resource and its cost-benefit evaluation was proposed.

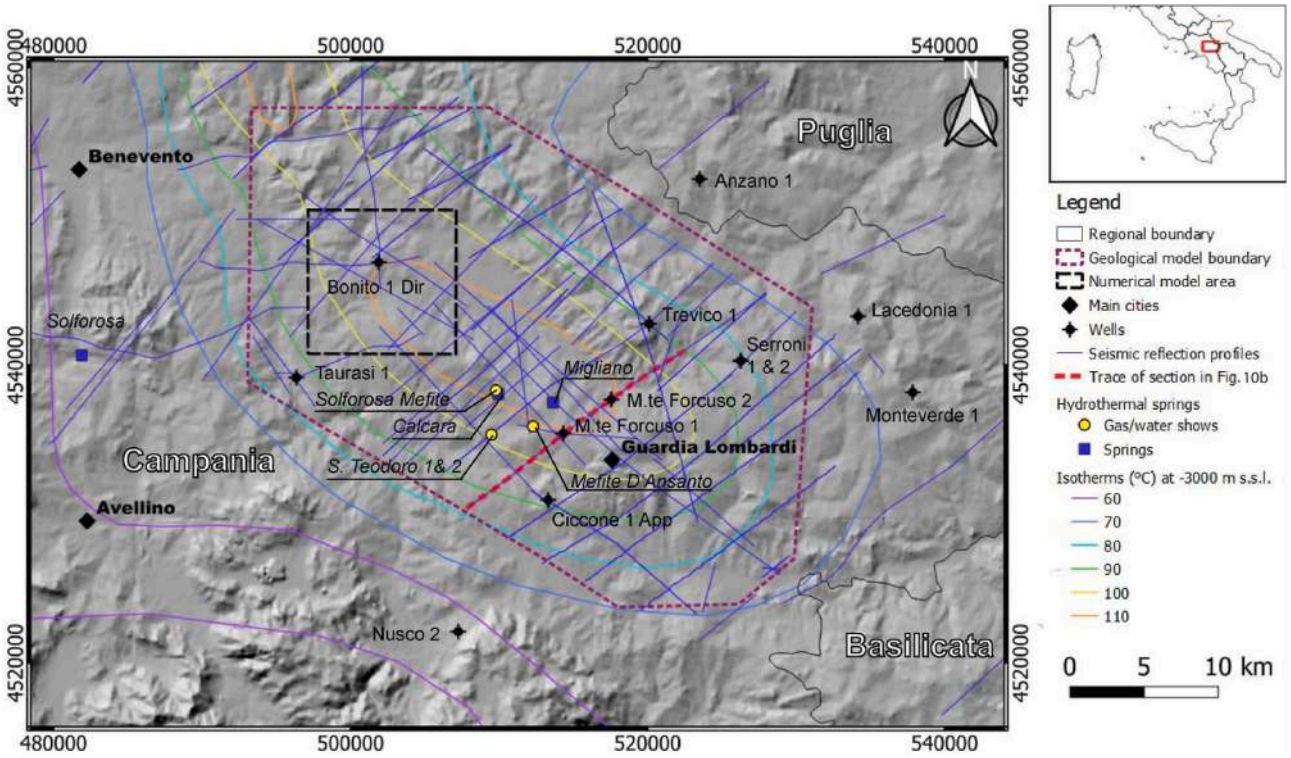

Fig. 1. Study area location map. The isotherms at −3000 m sub sea level, the hydrothermal springs, the locations of used data, the boundaries of the 3D geological and the numerical models, and the main cities are shown.

The case study proposed in this paper highlights how the exploration, evaluation and characterization of geothermal resources by using pre-existing subsurface data (mostly O&G), is not only possible, but also reduces costs, risks and technical timing, encouraging the harvesting of the geothermal resource. This represents a non-negligible factor in an era in which the adoption of measures aimed at containing CO_2 emissions is rather urgent.

2. Geological setting

The Guardia Lombardi area is located in the southern segment of the Apennines orogen [36,37]. This region is a fold-and-thrust belt developed in Neogene and Quaternary times along the eastward-retreating west-directed subduction of the Adria lithosphere [38–40].

The development of the Southern Apennines orogen occurred through the off-scraping and incorporation at the subduction zone of the Meso-Cenozoic sedimentary covers (essentially pelagic units and shallow water carbonates) located along the Adria passive margin and overlying active margin deposits [e.g., 17,20]. Different, and sometimes conflicting, palaeogeographical reconstruction have been elaborated for the passive margin of the Adriatic plate [41–46]. The main paleogeographic domains considered in this work are described in the following, in an order which corresponds to a west to east transect in the original paleogeography and from top to bottom in the cross-section in Fig. 2c (see Scrocca, 2010 [47] and references therein for details).

- Liguride-Sicilide nappes. These nappes derived from internal basinal units associated with the Ligurian-Piedmont branch of the Neotethyan Ocean. This group of units is composed by: i) the Early Cretaceous to Early Miocene Liguride units [48–51], which incorporated ophiolitic suites and which also comprises some metamorphic units (Frido Unit) and ii) the Late Cretaceous – Early Miocene basinal deposits of the Sicilide units [48].
- Apennine carbonate platform, made up of a thick pile (up to 5000 m) of shallow-water carbonates Late Triassic-Early Miocene in age [52–54] All the thrust sheets derived from Apennine Carbonate Platform are generally detached along an intra-Triassic décollement

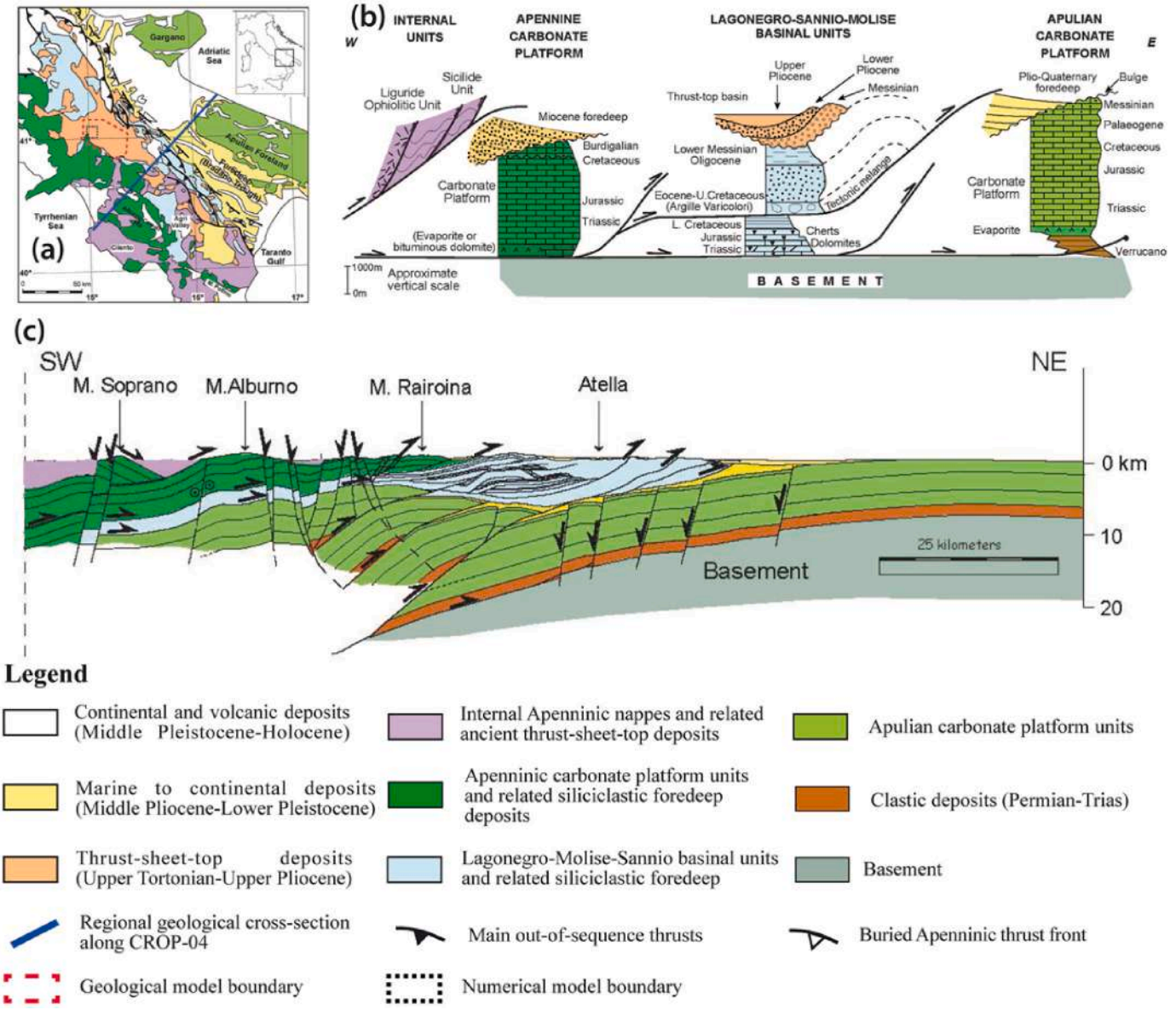

Fig. 2. Study area geological setting. (a) Simplified geological map of the southern Apennines. (b) stratigraphic scheme (c) and regional geological cross-section along the deep seismic profile CROP-04 (modified after Scrocca [47]).

from their Paleozoic substratum, which has never been reached by exploratory wells.

- Lagonegro-Sannio and Molise units. The Lagonegro unit is made up of Middle Triassic-Early Cretaceous basinal formations [55,56] and a still debated Late Cretaceous-Cenozoic section. The so-called Sannio Unit likely represents the Late Cretaceous-Early Miocene upper portion of the Lagonegro units, which was detached from the underlying Mesozoic portion and transported farther east [20,57,58]. The Molise basinal units, which outcrop along the eastern side of the Southern Apennines, are made up by Cenozoic deposits that have been detached from their original substratum and may be considered the remaining easternmost portion of the Lagonegro–Molise basin [42,44,59].
- Apulian carbonate platform. This unit crops out in the Apulia region foreland area [60]. It is made up of Upper Triassic-Miocene shallow-water carbonates, approximately 5000–7000 m thick (Fig. 2).

Mesozoic extensional tectonics dominated the regional paleogeography, resulting in the opening of the East Mediterranean and Ligurian-Piedmont (also known as Alpine Tethys) oceanic domains. According to the adopted model, the Apennine and Apulian carbonate platforms, as well as the intervening Lagonegro-Molise basin, evolved along the Adria passive continental margin, while the Liguride-Sicilide nappes are considered relics of the Ligurian-Piedmont oceanic domain. The Mesozoic Lagonegro-Molise basin may have represented the northern marginal region of the East-Mediterranean portion of the Neotethyan ocean [61,62], likely situated on thinning continental crust.

In the Southern Apennines, contractional deformation progressively propagated eastwards towards the foreland, incorporating slices of the Meso-Cenozoic sedimentary cover with well-documented thrusting events [38,63]. Since the middle Miocene, tectonic accretion within the thrust belt was followed by extensional backarc tectonics which crosscut the thrust pile, causing a thinning of the internal sectors of the belt [38,42,64,65].

The resulting overall structural setting of the Southern Apennines, shown in Fig. 2, is quite well defined by the available surface and subsurface dataset down to a depth of about 10 km [17,18,20,42,46,59,66,67,68]. Several significant differences exist, however, regarding the possible reconstructions of the deeper portion of the thrust belt which consider both thin-skinned and thick-skinned tectonic styles [47,69–72].

In this regional context, the local structural setting of the “Guardia Lombardi” area is characterized by the emplacement of thrust sheets, made up by slices of the Lagonegro-Molise basinal units, over a buried antiformal stack, developed within the Apulian carbonates in Pliocene times. The thrust pile was then offset by mainly extensional faults during Pleistocene times [20,30,49,50,68,73–76] (Fig. 2).

3. Data and methodology

3.1. Available datasets

This study is based on the integration, analysis and interpretation of subsurface data (i.e., well data and seismic reflection profiles) acquired in the study area for O&G exploration purposes and deriving from both public and confidential databases. Public data, consisting of some composite well logs and seismic reflection profiles in low quality raster format, derive mostly from the public ViDEPI database [77] and in part from some published papers and technical reports [27–35]. Confidential data, consisting of some composite well logs, well-core data, seismic reflection profiles in raster and/or SEG-Y digital format, were made available under a confidentiality agreement between the Italian National Research Council (CNR) and the ENI S.p.A. oil company.

The available public data were mainly used in the preliminary phases of our work and allowed us to define the geothermal potential of the study area subsurface, while confidential data, more numerous and detailed, were used in the subsequent phases to better define and characterize the geothermal reservoir and to perform a numerical simulation for evaluating its exploitation potential.

Data from deep wells (Fig. 3; Table 1), including geophysical logs (e.g., Spontaneous Potential, Resistivity, Sonic logs, etc.), stratigraphies, temperatures, drilling mud losses, cuttings, geo-fluid characteristics, well test (i.e., drill stem test, DST) results and some technical reports on the results of some well data analysis (e.g., chemical and geochemical analyses of gas, water and/or hydrocarbons) were analyzed. Four wells, such as Monte Forcuso 1, Monte Forcuso 2, Bonito 1 Dir and Ciccone 1, reach the geothermal reservoir and for three of them (i.e., Monte Forcuso 1, Monte Forcuso 2 and Bonito 1 Dir) the ENI company also provided the associated well-cores.

The reservoir 3D modeling, instead, is based on the analysis, elaboration and interpretation of 58 seismic reflection profiles acquired from 1976 to 1996 (Fig. 3) and made available by the ENI company. Most of them (30 profiles) are both in stacked and migrated version, the remaining seismic profiles are in stacked (23 profiles) or migrated (5 profiles) version. All profiles were provided in vectorial (SEG-Y) format and 7 of them were also provided in paper copy format. Since the seismic reflection profiles derive from different survey campaigns, they are characterized by different quality (from low to medium) and different datum plane elevation values (i.e., 400 and 500 m a.s.l.).

Once collected, all data were first quality-checked, homogenized in terms of graphical quality, as much as possible, and geo-referenced to a common spatial reference system (i.e., WGS 84/UTM zone 33N; EPSG:32633) using GIS software. Finally, seismic reflection profiles and well data were uploaded into a 3D environment using geological and geophysical modelling software (Fig. 3).

Since the datum plane elevation of most of the collected data was at 400 m a.s.l., the reference plane elevation of well and seismic data was set at this elevation.

As previously described, the data used in this study derives from pre-existing sources of different quality. While efforts were made to select the most reliable data, it is important to acknowledge that differences in acquisition parameters, processing techniques, data resolution, and original data formats (SEG-Y or paper copy formats) may have introduced biases in the seismic interpretation and in the characterization of geothermal parameters derived from well data. For example, seismic reflection profiles with lower resolution may obscure small-scale geological features, potentially affecting the accuracy of structural reconstruction. Similarly, well data with limited or inconsistent logging intervals could lead to some degree of uncertainties. To address these challenges, we integrated data from multiple sources and applied cross-validation techniques to enhance the robustness of our conclusions. However, we recognize that some assumptions were necessary during the analysis, and these could influence certain aspects of the results. Future studies could further reduce potential biases, in particular by incorporating more consistent well data.

3.2. Well data analysis

Well data analysis was essential to calibrate the seismic dataset with well stratigraphy information, to define the subsurface stratigraphic setting and to assess relevant rock properties (e.g., temperatures, presence of fracture systems and faults, fluid composition and pressure, etc.). These parameters are fundamental for evaluating the geothermal potential of the study area. For this purpose, in addition to the well location (e.g., well head coordinates, rotary table elevation, total depth, deviation survey, etc.) and stratigraphy (i.e., formation tops and lithologies) information, the main rock properties (e.g., temperatures, geo-fluid composition and pressure, etc.) were also incorporated into our database. The main results of the well data analyses are described below.

At first, as it represents the primary condition in choosing the investigation site, an accurate well stratigraphy analysis was carried out to identify the presence of potential reservoir rocks underlying possible

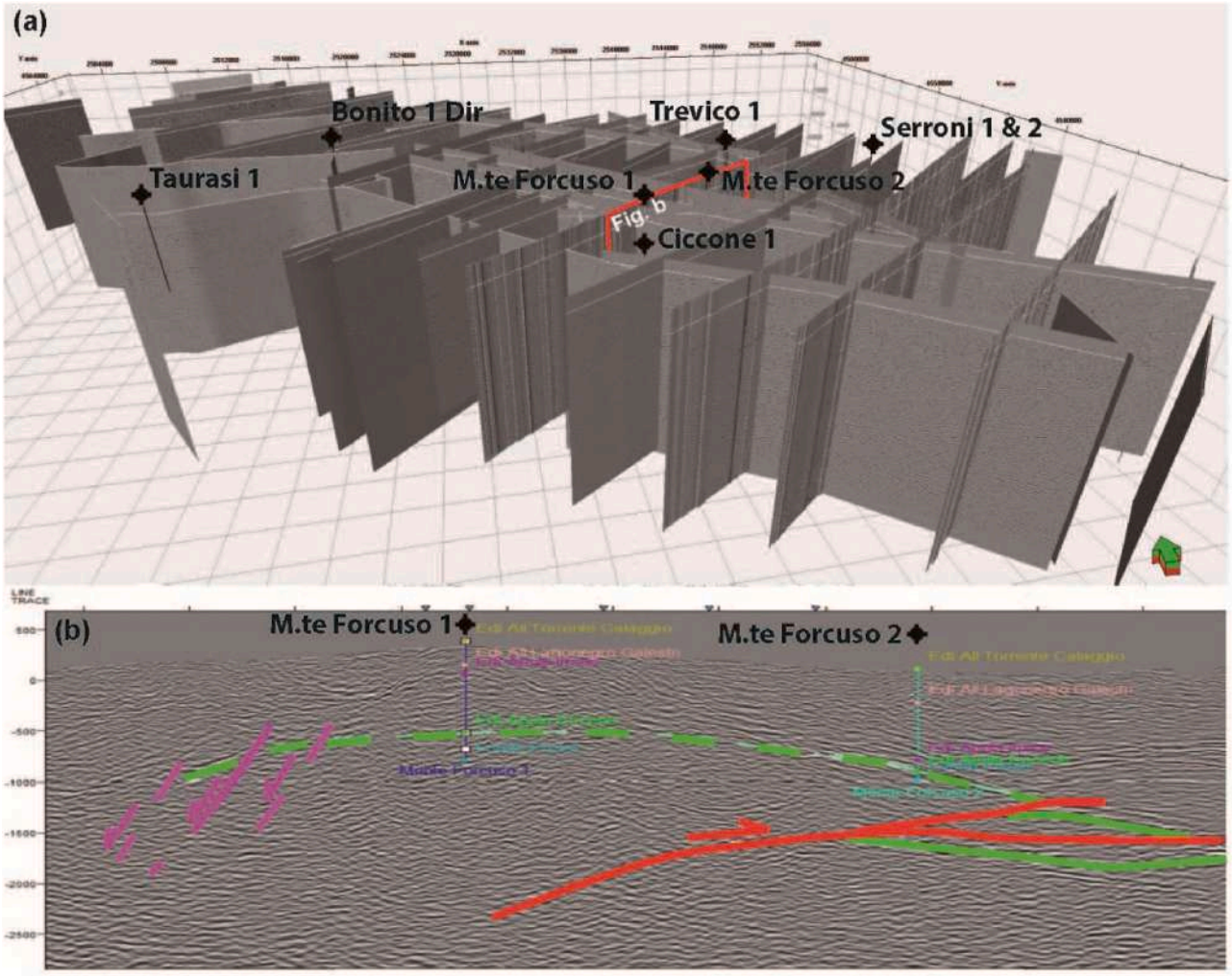

Fig. 3. Used dataset. (a) 3D view of the used seismic reflection profiles and wells; (b) Interpreted seismic reflection profile through the Monte Forcuso 1 and Monte Forcuso 2 wells (location in figure a). The geothermal reservoir top (green lines), the main thrusts (red lines) and some normal faults (fuchsia lines), as well as the well positions and the intercepted formation tops, are shown. Data locations in Fig. 1. Detailed well data in Table 1. (For interpretation of the references to colour in this figure legend, the reader is referred to the Web version of this article.)

Table 1
Available wells in the study area. Location map in Fig. 1.

Well name	Drilling year	Easting WGS84 UTM 33N	Northing WGS84 UTM 33N	Status	RTE (m)	TD (m)	Top Apula reservoir (MD in m)	Source
Bonito 1 Dir	1979	501849	4546998	Dry	566	3107	2565	ViDEPI
Ciccone 1	1979–1982	513278	4531037	Dry	731	2673	2497	[77]/ENI
M.te Forcuso 1	1961	514298	4535510	Dry	879	1800	1128	
M.te Forcuso 2	1963	517530	4537768	Dry	533	1690	1366	
Serroni 1	1957–1958	526260	4540384	Dry	849	2486		
Serroni 2	1958	526260	4540370	Gas	848	802		
Taurasi1	1989	496373	4539245	Dry	339,8	3476	3367	
Trevico 1	1960	520075	4542864	Dry	989	1561		

cap rocks (Fig. 4). The analyzed well stratigraphy information mainly derives from the well composite logs and, for some of them (Monte Forcuso 1, Monte Forcuso 2, Bonito 1 Dir and Ciccone 1), also from the study of the available well-cores.

For those wells in which potential reservoir and cap rocks were identified (i.e., Monte Forcuso 1, Monte Forcuso 2, Bonito 1 Dir and Ciccone 1), an updated correlation scheme was finally created (Fig. S2 in supplementary material).

To estimate the geothermal potential of the study area subsurface, the well temperatures reported in composite well logs and technical reports were analyzed. Since the available bottom-hole temperatures (BHTs) were recorded soon after cessation of drilling (dynamic conditions), as in most of the hydrocarbon exploration wells, they reflect the thermal conditions of the drilling mud, which generally cools the rocks around the borehole walls. Therefore, a correction was applied to extrapolate these temperatures to static conditions (static bottom-hole temperature, SBHT). Given the quality and the quantity of the available data, we applied an empirical approach for temperature correction, using a linear equation that considers the geothermal gradient of the area, which is of about 15–17 °C/km (for more details see Della Vedova et al. [27] and Förster et al. [78]). The used correction method is affected by an error of around 10 % and its reliability was verified by

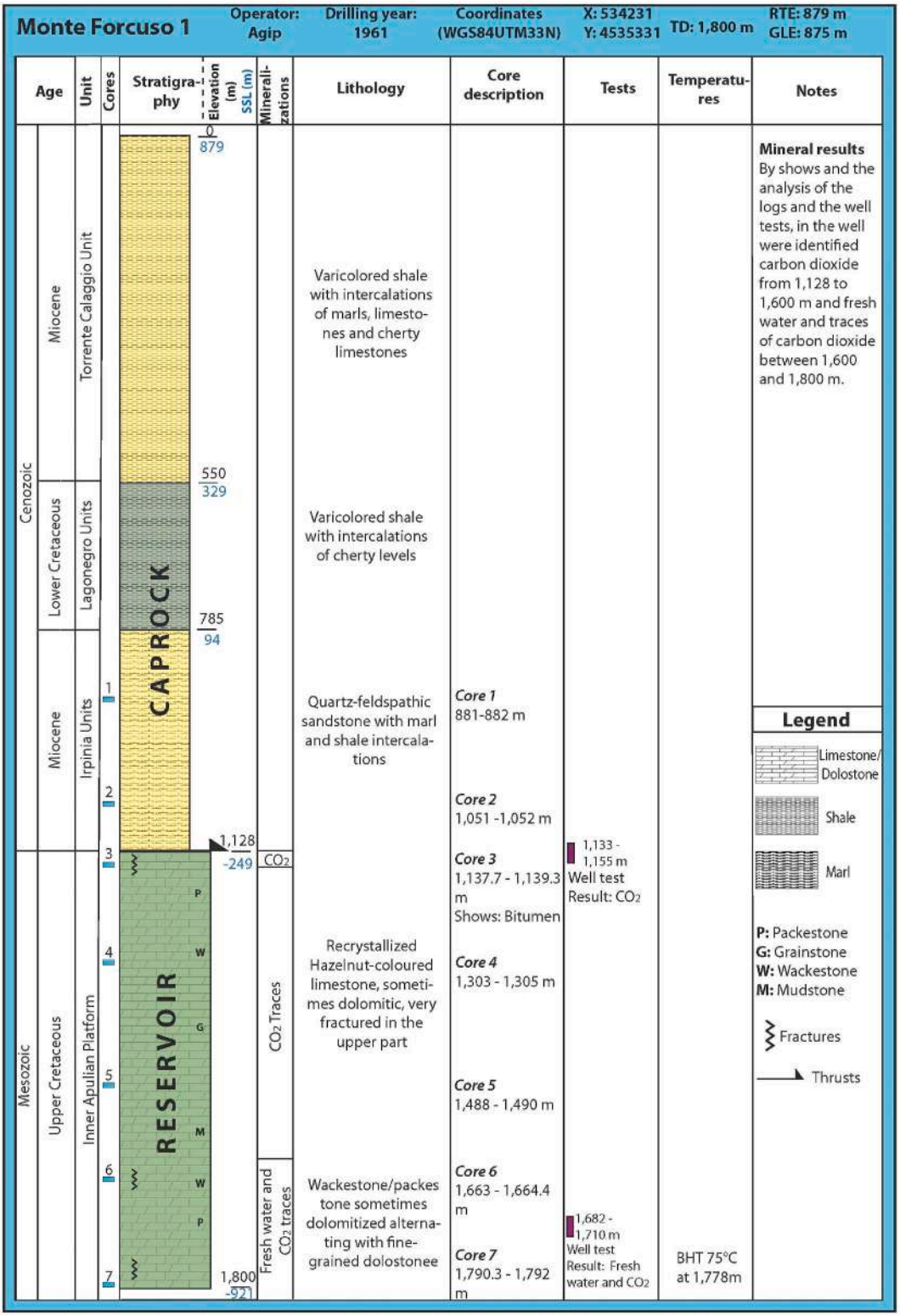

Fig. 4. Stratigraphic profile of Monte Forcuso 1 well. The stratigraphic intervals constituting the main geothermal reservoir (fractured carbonate rocks of the Apulian Platform; green colour) and the cap rocks (yellow and grey colours) are highlighted. Information about lithology, well-cores, well tests, temperatures and mining results are also reported. For more details on the carbonate interval see Fig. S1 in supplementary material. (For interpretation of the references to colour in this figure legend, the reader is referred to the Web version of this article.)

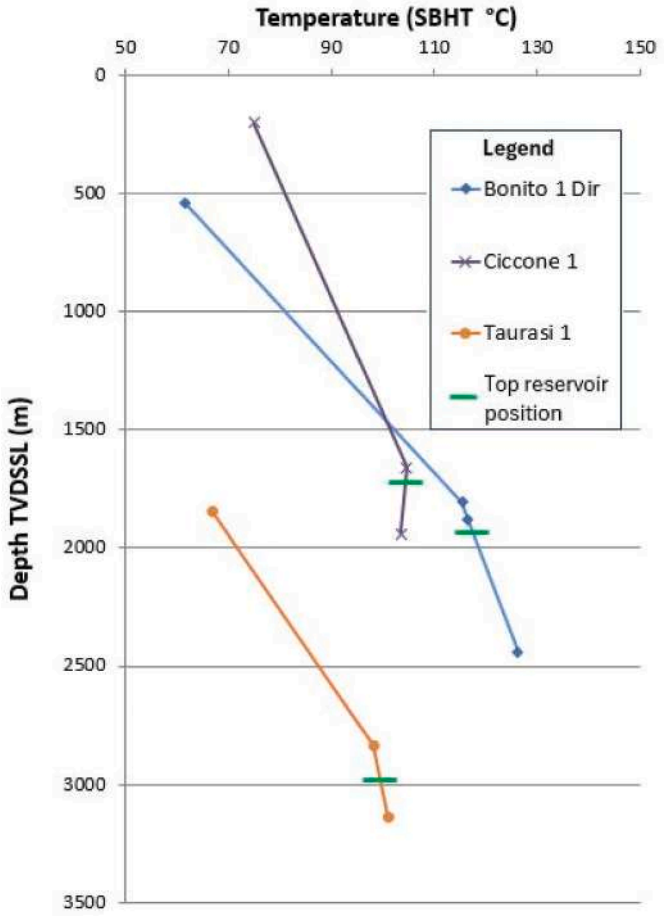

Fig. 5. Corrected temperatures. Graph of the static bottom-hole temperatures (SBHTs) extrapolated for some wells drilling the geothermal reservoir in the investigated area (i.e., Bonito 1 Dir, Ciccone 1, and Taurasi 1). Green dashes represent the position of the geothermal reservoir top within wells. Depths are expressed in meters below sea level (True Vertical Depth Sub Sea Level, TVDSSL). Well location in Fig. 1; well temperature data in Table 2. (For interpretation of the references to colour in this figure legend, the reader is referred to the Web version of this article.)

comparing the extrapolated SBHTs (Fig. 5; Table 2) with temperature values determined on thermal waters using geothermometers [35].

For Monte Forcuso 1, Monte Forcuso 2, Ciccone 1 and Bonito 1 Dir wells, we analyzed the mud loss values recorded in their deeper portions, within the Apulian carbonate rocks, to detect possible fracture systems and faults relevant for fluid circulation.

The interpretation of mud loss values was carried out using a standard mud viscosity of 25 cP; this value is also reported in some well logs. As an example, Fig. 6 shows the mud loss values, together with the well-core and the hydraulic well test (Drill Steam Test, DST) positions, at the bottom portion of Monte Forcuso 1, Monte Forcuso 2 and Bonito 1 Dir wells.

This analysis, combined with the DST results, also allowed us to determine the permeability (K eff) values of the fractured intervals within the carbonate units. It is important to note that, since both drilling speed and thermal correction data were not available, permeability values derived from mud losses are not highly accurate. It should be specified that, due to the drilling mud high viscosity, the permeability values derived from the mud loss values are generally lower than the permeability values derived from DSTs (Fig. 7; Table 3).

The analysis of well-cores from Monte Forcuso 1, Monte Forcuso 2 and Bonito 1 Dir wells provided further qualitative information on the fracture systems, faults, and lithologies (Fig. 8, Table 4). They consist of both whole portions (maximum length about 30 cm) and incoherent and considerably fragmented material (Fig. 8). Since well-cores are not oriented and often fragmented, it was not possible to define the orientation of the observed discontinuity structures, either sedimentary (e.g., laminations, layer surface, etc.) or structural (e.g., joints, PSS, faults). For these reasons, we defined the geometry of the main fault systems only by means of the seismic profile interpretation.

The core plugs were used by ENI lab to calculate the rocks porosity (Phi in Table 4), but since the recovery factor of well-cores in the reservoir is very low, for assigning the properties of permeable zones, we relied on hydraulic testing and estimation from mud losses. In our approach, we used a Darcy integrated equation whose results are reported in Table 3 for the most reliable tests, with major uncertainties on viscosity values. This is due to a basically unknown temperature of the fluid during the hydraulic tests, salinity correction of viscosity and presence of drilling mud in the fluids.

Regarding to porosity, what generally is accepted is 1–5% porosity for a compact limestone with a percentage ranging from 0.5 up to 3 % for micro fracturing. In the core plugs, however, far higher values were observed without considering the not-recovered samples. In a relatively optimistic assumption, we may safely assign the average of the maximum porosity values observed as porosity of the damage zone in the reservoir (nearly 5 %).

3.3. *Seismic interpretation and 3D geological modelling*

The 3D geological reconstruction of the potential geothermal reservoir is based on the seismic dataset interpretation, constrained with well data. In detail, we first interpreted the faults and correlated them to identify the various sub-volumes into which they divide the model volume. After, the Apulian Carbonate Platform top was interpreted.

The interpreted seismic horizon was identified by calibrating the seismic profiles with the well stratigraphy data (Fig. 3b) and by observing the different seismic facies, where allowed by the quality of the seismic profiles. Given its high acoustic impedance contrast, the top of the Apulian Carbonate Platform was interpreted in the whole study area. Finally, the interpreted reservoir top horizon was joined with the related well tops and gridded using a “convergent interpolation” algorithm. In this way, we obtained a 3D surface in two-way times separating the cap rock and the reservoir units (Fig. 9a).

Afterwards, the 3D model in two-way times was depth-converted applying a 3D interval velocity model derived from the well data (Fig. 9b) and 3D model in depth of the study area subsurface (Fig. 9c and d) was obtained.

4. Characterization of geothermal resources

By means of the analysis of well stratigraphies the area subsurface can be subdivided into two main lithological intervals, such as: the carbonate rocks (Cretaceous-Eocene time), belonging to the Carbonate Apulian Platform, and the marly-clayey rocks, belonging to the allochthonous (i.e., from bottom to top: Irpinia Unit, Daunia Unit, Lagonegro Unit, Sannio Unit and Torrente Calaggio Unit) and the

Table 2
Available well temperatures. In this table the following information are shown: well name, rotary table elevation (RTE), ground level elevation (GLE), well total depth (TD), true vertical depth sub sea level (TVDSSL) of the top Apula reservoir, lithology where the measurement point falls, TVDSSL of the measurement point, measured temperature, corrected temperature (SBHT), temperature correction method and source data. All the elevation and depth data are expressed in metres.

Well name	RTE (m)	GLE (m)	TD (m)	Top Apula reservoir TVDSSL (m)	Lithology	Measurement depth TVDSSL (m)	Measured temperature (°C)	Corrected temperature (°C)	Temperature correction method	Data source
Bonito 1 Dir	566.2	560	3107	−1918,9	Cap rock	537.8	57	61.4	Della Vedova [27] 15–17 °C/km	ENEL [28]
					Cap rock	1806.8	105	115.4		
					Cap rock	1881.8	106	116.5		
					Apula reservoir	2440,8	118	126.2		
M.te Forcuso 1	879	875	1800	−249	Apula reservoir	899	75	83		
M.te Forcuso 2	533	529	1690.5	−832	Apula reservoir	1155	87	96		
Ciccone 1	731	725	2673	−1894	Cap rock	199	67,5	74.9		ENI S.p. A.
					Cap rock	1660	95	104.6		
					Apula reservoir	1940	94	103.6		
Serroni 1	848.8	845	2486		Cap rock	394.25	41	46.3		ENEL [28]
					Cap rock	1635.25	65	72.2		
Taurasi 1	339.8	331	3476	−2978.2	Cap rock	1846.2	60	66.8		ViDEPI [77]
					Cap rock	2837.2	89	98.2		
					Apula reservoir	3136.2	96	101	Horner Plots	
Trevico 1	988.7	985	1561		Cap rock	115.3	40	45.2	Della Vedova [27] 15–17 °C/km	ENEL [28]

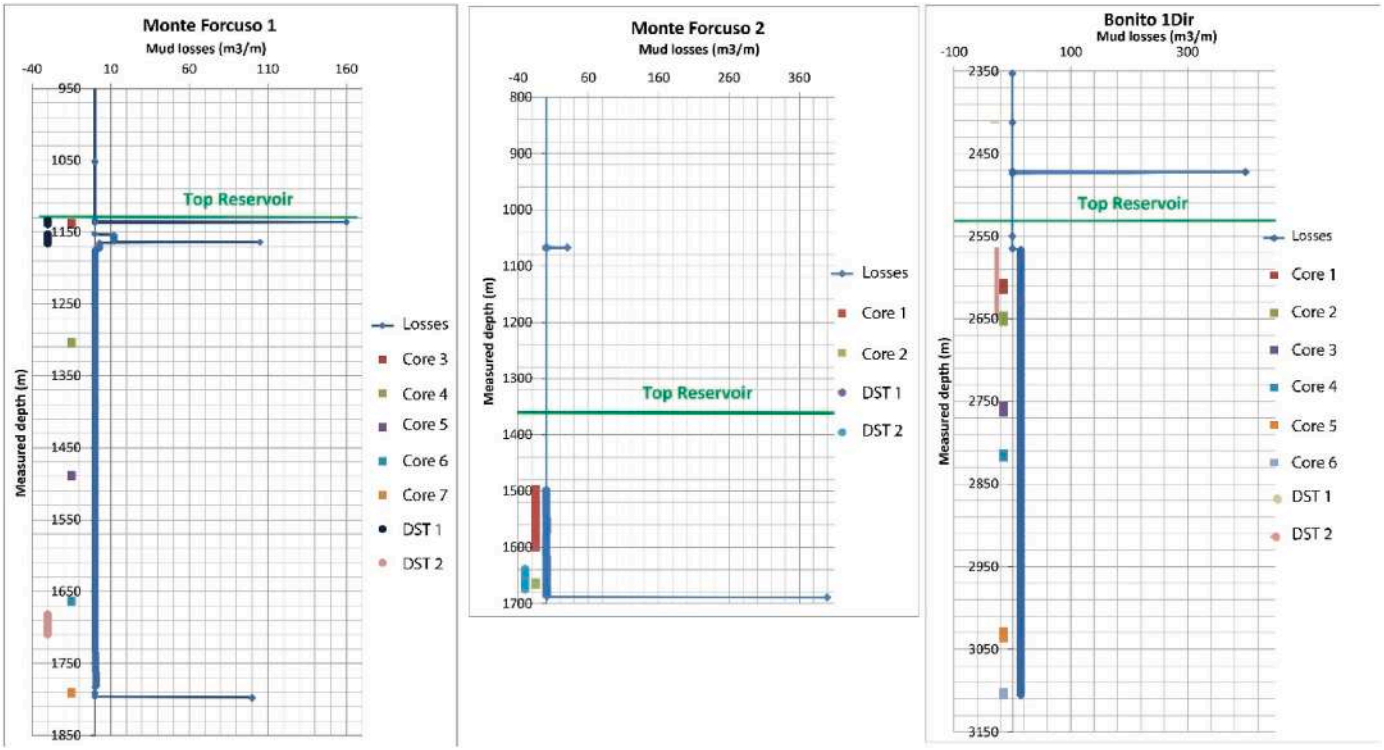

Fig. 6. Drilling mud losses. Drilling mud losses of Monte Forcuso 1, Monte Forcuso 2 and Bonito 1 Dir wells. The position of well-cores and well tests (DST) are also reported in the graphs.

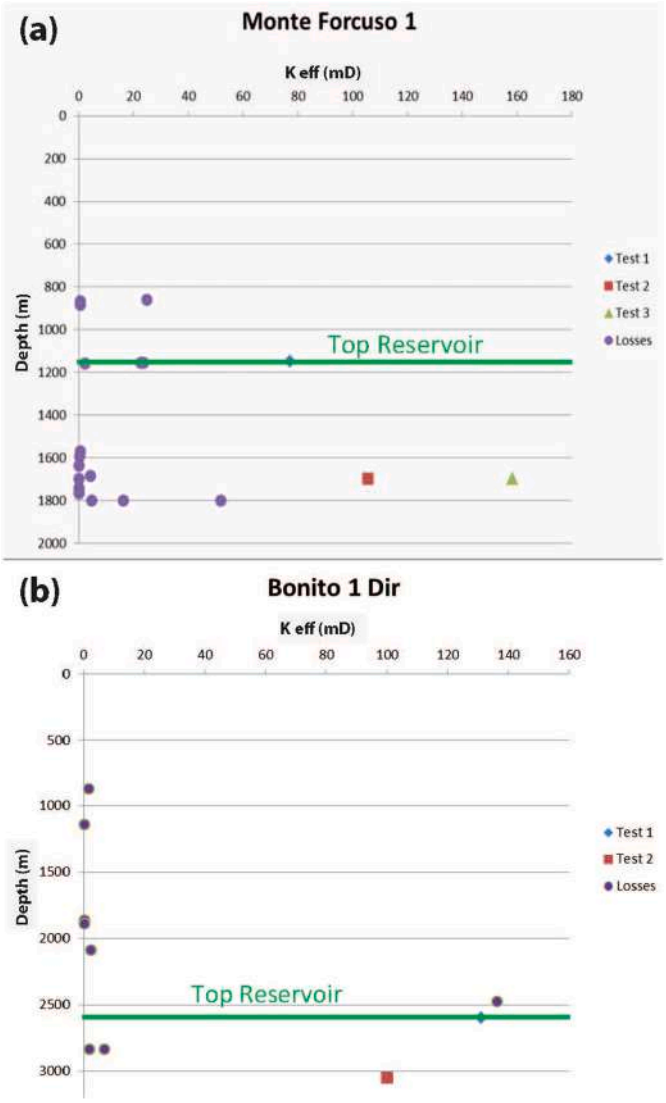

Fig. 7. Poro-permeability data. Permeability (K eff) estimates (in millidarcy, mD) in (a) Monte Forcuso 1 and (b) Bonito 1 Dir wells deriving from the values of the drilling mud losses (purple dots) and DST results (other variously colored symbols; Table 3). The dots are centered on the tested levels. The top reservoir position (green line) is also shown. (For interpretation of the references to colour in this figure legend, the reader is referred to the Web version of this article.)

Pliocene units (Fig. 4).

The interpretation of the seismic dataset and the 3D geological modeling of the carbonate unit top revealed the presence in the study area subsurface of a wide anticline affecting the carbonate rocks and set above NE-verging thrusts belonging to the southern Apennine orogenic wedge (Fig. 10). These thrusts consist of several NW-SE-oriented splays converging at depth while the highest one shows an arched front separating two different structural culminations (Fig. 10a). The higher and wider structural culmination is intercepted by Monte Forcuso 1 well at a depth of 1125 m below the ground level (−250 m sub sea level), while the smaller and deeper one is intercepted by Bonito 1 dir well at 2315 m below the ground level (−1750 m sub sea level). The backlimb of the Monte Forcuso structural culmination and the overlying allochthonous units are dislocated by three NW-SE-oriented and SW-dipping high-angle normal faults, the innermost of which, known as Mefite D'Ansanto Fault System, intercepts the CO_2 accumulation that occupies the Monte Forcuso structural culmination (Fig. 10b).

In correspondence with the Monte Forcuso culmination, the

Fig. 8. Some examples of available reservoir well-cores provided by ENI. Cores consist of both blocks and incoherent material, due to the intense state of fracturing in the interval in which the core was taken. In the intact blocks, the circular holes correspond to the core plugs on which porosity and permeability measurements were performed.

Table 3
DST results. Evaluation of the results of the most reliable DSTs done by using integrated Darcy equation.

Well name	Top (MD m)	Bottom (MD m)	Produced Fluid (m^3)	Produced Fluid (type)	Static Pressure (kg/cm^2) Before or after Hydraulic testing	Delta Pressure for Testing (kg/cm^2)	Timespan (minutes)	Diameter (in)	K eff (mD)	Flow (l/min)
M.te Forcuso 1	1682	1710	6.16	Water	196	88	30	11	158.2	205.33
M.te Forcuso 2	1538	1572,5	2.72	Mud first and water	nd	57	35	5	165.08	77.71
Bonito 1 Dir	2996	3107	5.25	Muddy water	174,2	37.8	523	5	99.9	10.04
Ciccone 1	2403	2456	330	Water	194,4	187.4	3465	5	40.1	95.24

Table 4
Core plugs data. Available porosity (Phi) and permeability (K eff) data from core plugs within the geothermal reservoir, courtesy by ENI.

Well Name	Core Number	Top (MD m)	Bottom (MD m)	Formation/Age	Phi Min (%)	Phi Max (%)	K eff (mD)	Source
M.te Forcuso 2	1	1497.5	1500	Apulian Platform/Lower Cretaceous	7.6	8.8	<0.1	ENI
Bonito 1 Dir	2	2646	2655	Apulian Platform/Middle Eocene	0.38	1.74	2,33	ENI
	3	2755	2764		1.01	10.29	1.86	
	4	2813	2818		0.33	9.79	0.1	
	5	3030	3037	Apulian Platform/Lower Senonian	0.21	0.92	0.3	
	6	3102	3107	Apulian Platform/Turonian-Senonian	0.24	4	<0.1	
Ciccone 1	5	2495	2504	Brecce di Lavello/Upper Paleocene	0.52	1.83	0.3	ENI
	8	2664	2664.7	Calcare di Cupello/Cenomanian	0.47	2.34	<0.1	

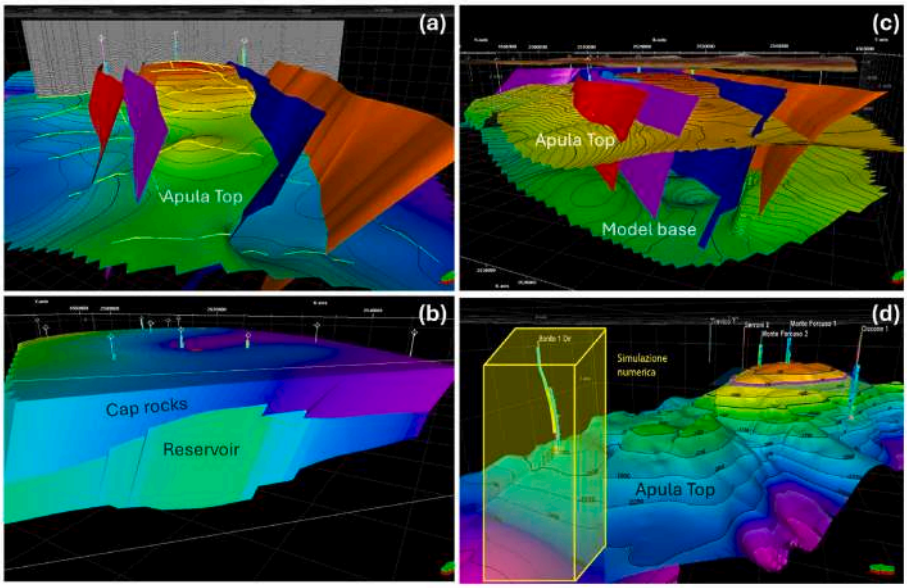

Fig. 9. 3D geological model. (a) 3D view in time domain of the Apulian Carbonate Platform top (Apula top) and the fault surfaces (high-angle variously colored surfaces). A seismic reflection profile (in grey colour), the traces of the interpreted seismic profiles (yellow lines) and the well positions are also shown. (b) 3D Velocity model used for the dept-conversion. The well positions (white symbols) are shown. (c) 3D view in depth domain of the Apulian Carbonate Platform top (Apula top) and the fault surfaces. The depth-converted model base is also represented. (d) 3D view of the geothermal reservoir top (Apula top). The isobaths are expressed in meters above sea level. The main wells with the associated geophysical logs (resistivity on the right and spontaneous potential on the left), the CO_2/water contact at the structural culmination intercepted by the Monte Forcuso 1 well (fuchsia polygon) and the volume interested by the numerical modelling simulation (yellow parallelepiped) are represented. The image is vertically exaggerated. (For interpretation of the references to colour in this figure legend, the reader is referred to the Web version of this article.)

geometry and the extension of the CO_2 accumulation were also defined. It consists of a CO_2 gas cap with a maximum thickness of approximately 470–500 m in the culmination area. This gas cap is not encountered by the surrounding deep wells (i.e., Monte Forcuso 2, Bonito 1 Dir, Ciccone 1 App), which intercept the underlying brackish water deep aquifer (Fig. 10b).

Well data analysis made it possible to define the main subsurface characteristics, particularly those of the carbonate unit.

The SBHT values, extrapolated with the empirical correction of the measured bottom well temperatures (BHTs), highlight the presence of a geothermal anomaly in the study area, with temperatures reaching ~125 °C at −2300 m sub sea level in correspondence with Bonito 1 Dir well (Fig. 5), within the geothermal reservoir. The extrapolated SBHTs result quite similar with temperature values reported in Duchi et al. [35] and determined on thermal waters using geothermometers.

The drilling mud loss values, instead, suggest the presence of several fractured intervals within the carbonate units intercepted at the bottom portion of Monte Forcuso 1, Monte Forcuso 2, Ciccone 1 and Bonito 1 Dir wells.

The analysis of mud losses suggests permeability values ranging between 0.1 and 50–60 mD, while well test results provided higher effective permeability values ranging between 100 and 135 mD in Bonito 1 Dir well and between 80 and 160 mD in Monte Forcuso 1 well (Fig. 7, Table 3). Differently, some tests carried out by ENI company on undamaged rock samples (core plugs) gave low porosity (on average around 0.2–4%, with a few exceptions around 9–10 %) and permeability (0.1–5 mD) values.

Well tests also gave information on the chemical composition and the pressure of the intercepted geo-fluids. As an example, in Table 5 we report the chemical composition of some water samples from the carbonate unit within Bonito 1 Dir, Ciccone 1 and Monte Forcuso 2 wells. In Monte Forcuso 1 well the chemical composition of water samples suggests the presence of CO_2 from the carbonate top up to 720 m below sea level, where a CO_2-brackish water transition was intercepted. On the contrary, in Monte Forcuso 2, Bonito 1 Dir and Ciccone 1 deep wells only brackish water was intercepted.

5. Reservoir numerical simulation

Once the stratigraphic and structural setting of the geothermal reservoir was reconstructed, and its geothermal potential was defined, a specific numerical simulation of the geothermal reservoir behavior in correspondence with Bonito 1 Dir well was carried out. The software used for the calculation of the model is Petrasim v2020.1 [79], which is the most popular graphical interface for the family of TOUGH2 reservoir simulators, considered among the best in the world and developed by

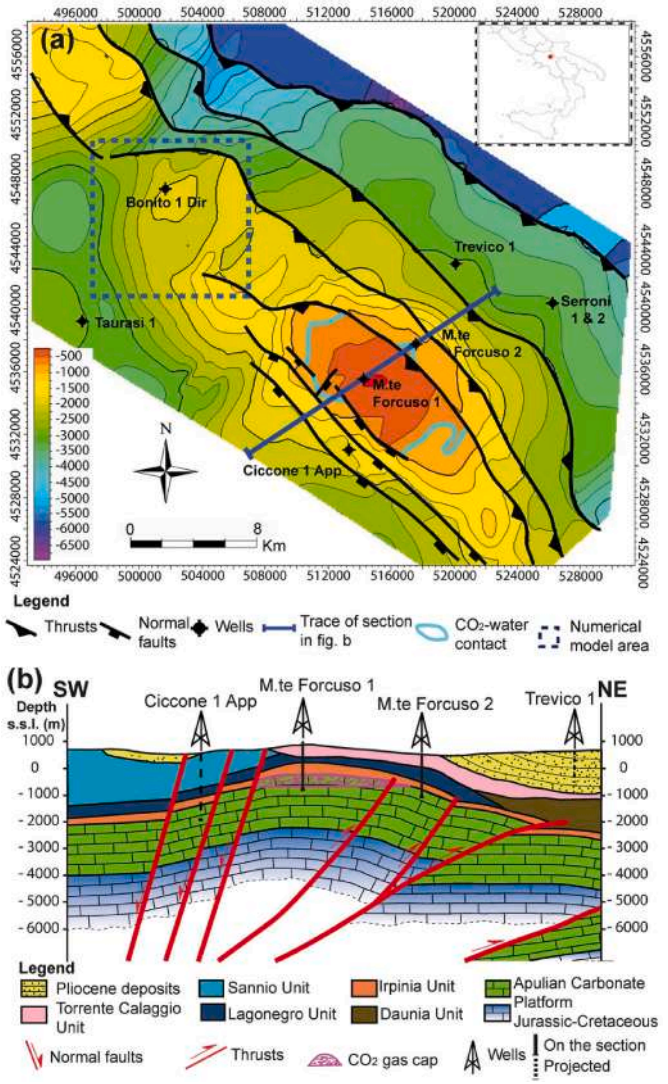

Fig. 10. Geothermal reservoir. (a) isobath map of the geothermal reservoir top (i.e., top of the Apulian Carbonate Platform); (b) SW-NE geological cross-section through the geothermal reservoir. Section trace in figure a. Elevation values (referred to sea level) are expressed in meters.

Lawrence Berkeley Laboratories. In particular, for this study TOUGH2 – EOS2 was used, with an equation of state able to simultaneously consider Water, Steam and CO_2.

The Monte Forcuso 1 well area was not considered due to the presence of the large CO_2 gas cap, which probably fuels the Mefite d'Ansanto CO_2 emission [33,80,81]. The thermal capacities of carbonates were used for the material definition, even considering the presence of fluids and their composition [82].

Once the numerical model volume, consisting of a 10 × 10 km large and 5 km deep parallelepiped, was defined, it was discretized with 106,650 cartesian meshes with local refinement in correspondence with Bonito 1 Dir well and the proposed production and injection wells, and populated with the temperature and pressure values deriving from wells. The model volume was divided into two main intervals separated by the reservoir top, such as: the reservoir, subdivided into 21 layers, and the cap rocks, subdivided into 6 layers (Fig. 11).

The boundary conditions were set at the top and bottom layers; the bottom layer was set at 130 °C and the top layer at 30 °C, accounting for

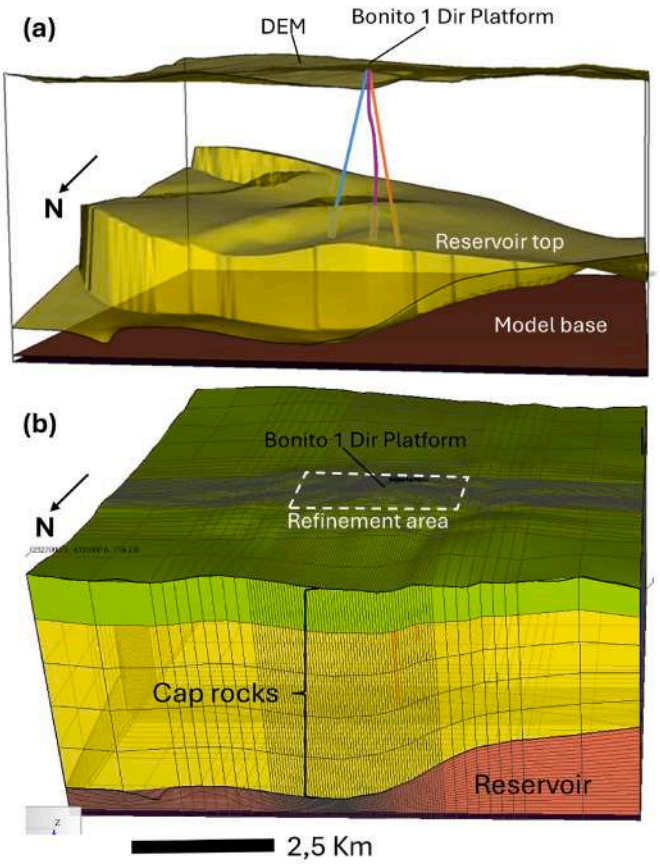

Fig. 11. Numerical model configuration. (a) layer configuration. From top to bottom the following layers are represented: digital elevation model (DEM), reservoir top and model base. The trajectories of Bonito 1 Dir well (fuchsia line) and the production (light blue line) and injection (orange line) wells are also shown. (b) Discretized 3D geological model. The cap rock and reservoir units are shown. The position of the Bonito 1 Dir well platform (from which the geothermal doublet starts) and the refinement area are also reported. For the numerical model location see Fig. 9d and 10a. (For interpretation of the references to colour in this figure legend, the reader is referred to the Web version of this article.)

Table 5
Geofluid compositions. Chemical composition of some water samples from some wells drilled in the study area.

Well name	Sampling date	pH	Recalculated pH	Salinity NaCl (g/l)	Measured depth (m)	Na (mg/l)	K (mg/l)	Mg (mg/l)	Ca (mg/l)	HCO_3 (mg/l)	Cl (mg/l)	SO_4 (mg/l)
Monte Forcuso 2	8/22/1963	7.15		2.48	1538–1572	1740	150	40	220	2380	1500	670
Ciccone 1	5/22/1982	7.9		4.167	2403–2456	2000	265	38	150	1709	2528	467
Bonito 1 Dir		8.01	8.1	0.877	2352–2412	577	19		37	488	532	284
	6/15/1979	7.23		4.03	2550–2646	2103	307	18	264	2288	2445	495
	January 07, 1979	6.57	4.96	3.51	2996–3107	1839	206	23	259	2380	2129	430

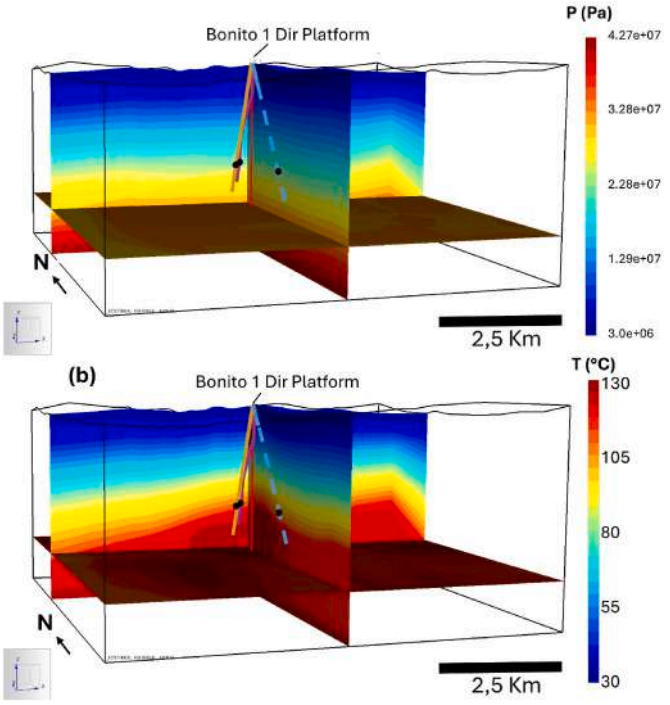

Fig. 12. Numerical model boundary conditions. (a) Pressure distribution within the numerical model volume. (b) Temperature distribution within the numerical model volume. The trajectories of the Bonito 1 Dir well (fuchsia line) and the production (light blue line; dashed behind the section) and injection (orange line) wells are shown. The reservoir top position intercepted by wells is indicated by black dots. (For interpretation of the references to colour in this figure legend, the reader is referred to the Web version of this article.)

the average yearly temperature corrected for the depth of the center cell in the first layer and constant flow. Although the presence of slightly overpressured shaly layers in the lower portion of the caprock has been detected, the geothermal reservoir shows a hydrostatic gradient [e.g., 24]. Accordingly, for the sake of simplicity, for pressure conditions, the first layer of the model was set at about 30 bar and the bottom layer at 426 bar, in order to reproduce the hydrostatic gradient recognized within the geothermal reservoir.

We applied these conditions to respect the hydrostatic pressure, identified with the hydraulic tests, but such as to compensate for the density variation due to the heat flow with an incoming/outgoing flow. We also included in the model the major solutes in the reservoir fluid and the partial CO_2 pressure. The porosity and permeability values obtained by means of hydraulic tests and well-core analysis were also considered.

At this point, we run the calculation until a stable state (steady state) was reached and compare the results with the well data; if the calculation failed, the boundary conditions were corrected, and the calculation was repeated until success. In Fig. 12 the pressure and temperature distribution are reported.

Once a stable state was reached, some virtual wells were introduced into the model to analyze the geothermal system response to the hypothesized extraction activities. Different extraction scenarios were modeled changing the mass flow rate, using an extraction well and a reinjection one (doublet scheme). The extraction and the reinjection wells consist of two deviations departing from the same well platform and diverging downwards up to a distance of about 2.5 km at the reservoir depth (Fig. 11).

We carried out several scenarios with mass flow ranging from 40 kg/s to 150 kg/s and lasting 30 years.

We considered the thermal problems due to the geothermal system cooled by the reinjection fluid and a rock volume from which heat can be extracted. In the presence of fractured rocks, as in our case study, it is difficult to define this volume because water does not permeate all the rock volume but only the portion surrounding the fractures, therefore heat can be extracted only from this limited rock volume. Since we did not have information about the fracture system of the study area, we decided to use average estimations of this parameter. From literature, we know that the statistical distribution models of the fractures provide an estimation of the percentage volume of rock involved in the heat exchange as a function of the average distance between the fractures and their size [83]. Grant and Garg [84] proposed a general estimation of around 10 %. Consequently, we carried out two scenarios with 10 % and 100 % heat recovery. For the reinjection temperature, instead, we adopted a value of 65 °C, corresponding to the temperature of a fluid produced in an electric power plant based on a secondary fluid at the lower operability limit. The reservoir behavior evaluation was carried out using a thickness of 600 m. In Fig. 13 the thermal conditions at 2300 m depth after 30 years of geothermal exploitation with different mass flows and heat recovery percentages are shown.

It is worth mentioning that in case of fluid reinjection the contribution of the fluid rising from the lower part of the geothermal reservoir must be considered. However, in our case study, the permeability and porosity values at the deepest reservoir portion was estimated for lithostratigraphic continuity, but we must consider that a different grain distribution in the carbonate rocks could significantly modify their porosity and permeability, so real values can only be obtained by carrying out well tests.

In the doublet scheme, due to the fluid reinjection into the geothermal reservoir, the extraction rates can be increased up to about 150 kg/s. This extraction rate, under the reservoir and simulation conditions, is sustainable for about 30 years (Fig. 13), but there could be some problems with thermal interference in case of low heat recovery factor; due to the relatively high permeability, the reinjection pressure does not increase more than 10 % the reservoir pressure in the studied conditions (Fig. 14). The same is not true with respect to thermal breakthroughs, and in the 150 kg/s we have the start of a thermal breakthrough at about 22.2 years, with a temperature drop of about 2 °C, while the cold plume does not reach the production well. This, however, is a risky situation, because a small permeability anisotropy could promote the thermal breakthrough, and the cold plume reaching the production well, at an earlier time. For this reason, to have some margin while dealing with permeability anisotropy, preferential pathway and thermal recovery factor (that are unknown) we suggest a flow rate of 70 kg/s maximum.

6. District heating application

Following the numerical model, a possible use of the detected geothermal resource and the most appropriate technology for its valorization is proposed considering the decarbonization goals and the local characteristics [85].

We focused on using geothermal energy integrated in an energy community for the growth of the local economy. Therefore, the proposed utilization of the geothermal resource is the district heating system for a nearby town. The selected candidate is Grottaminarda, a town with 7813 inhabitants in the Avellino province (Campania Region, Southern Italy), located 80 km northeast of Naples.

Grottaminarda town is characterized by a temperate climate in which cold winters alternate with mild summers. Snowfall is possible during the winter. Throughout the year, the temperature usually fluctuates from 2 °C to 30 °C and is hardly below −1 °C or above 34 °C [86]. Grottaminarda is in class D of the climate/energy italian classification area, consisting of 166 days of heating for 12 h per day [87].

The building's heritage in Grottaminarda can be described through the data collected with the census in 2011. The residential buildings are 1149 and 139 are commercial or public buildings. 98 % of the buildings consist of single-family homes and small condominiums of up to 8

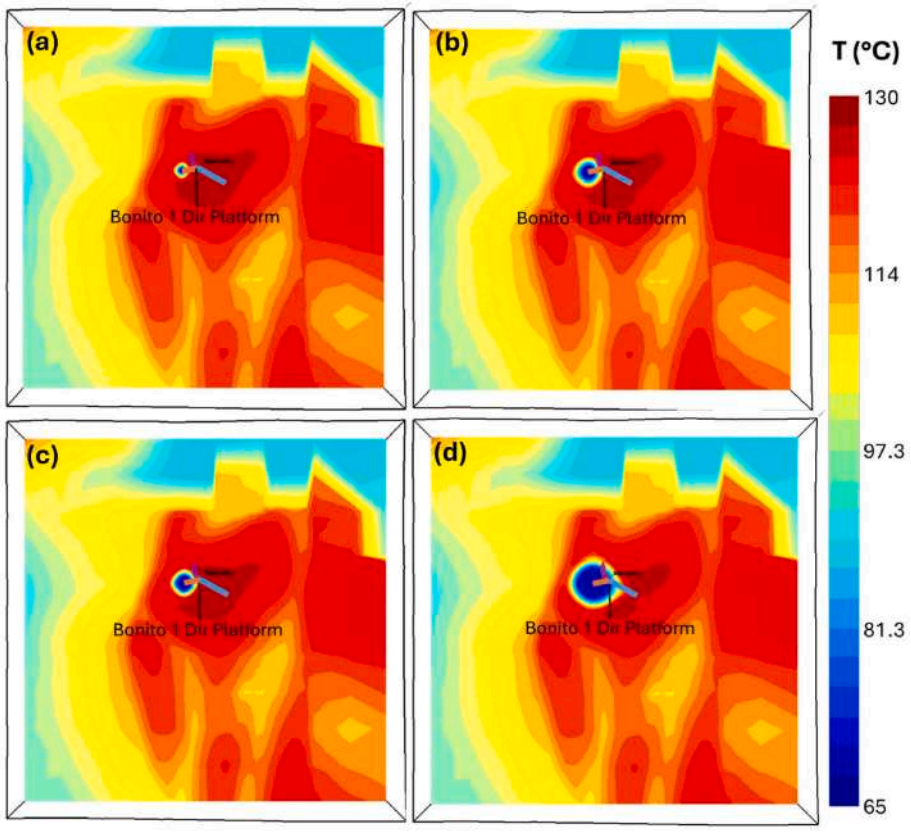

Fig. 13. Post-exploitation thermal conditions. View from above of the thermal plume at 2300 m depth after 30 years in the 40 kg/s mass flow scenario with (a) 100 % heat recovery and (b) 10 % heat recovery and in the 150 kg/s mass flow scenario with (c) 100 % heat recovery and (d) 10 % heat recovery. The trajectories on map of the Bonito 1 Dir well (fuchsia line) and the production (light blue line) and injection (orange line) wells are shown. (For interpretation of the references to colour in this figure legend, the reader is referred to the Web version of this article.)

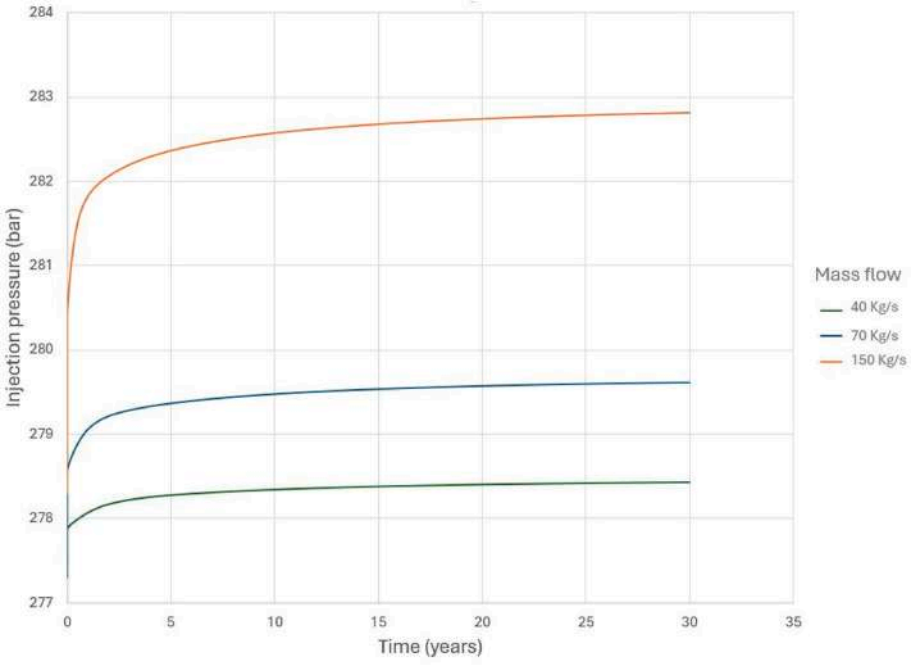

Fig. 14. Exploitation trends. The graph shows the injection pressure trend over time with different mass flows.

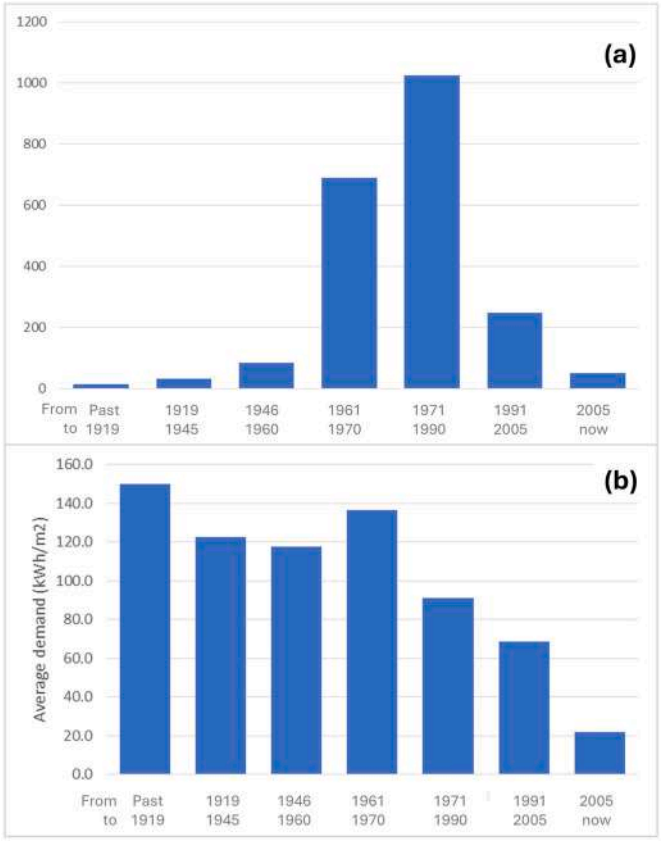

Fig. 15. Characterization of building heritage in Grottaminarda municipality. (a) distribution over time and (b) average energy demand by building period.

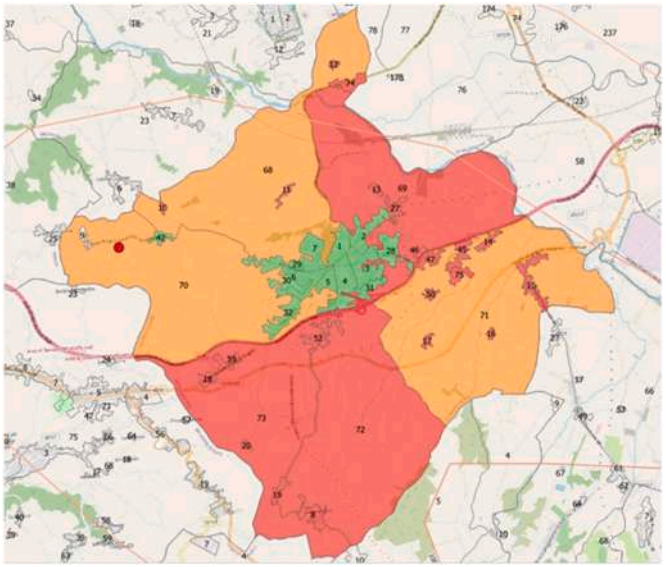

Fig. 16. The Grottaminarda municipality census section. In green, the sections with an inhabitant density larger than 1000 people/m^2; in orange and red, the inhabitants are less than 1000 people/m^2 and those are not included in the energy demand calculation. The red dot is the location of the well area. (For interpretation of the references to colour in this figure legend, the reader is referred to the Web version of this article.)

residential units, mainly built from 1961 to 1990 (Fig. 15). The calculated average demand, following the methodology discussed in Alimonti et al. [88], as a function of the building age highlights the decreasing

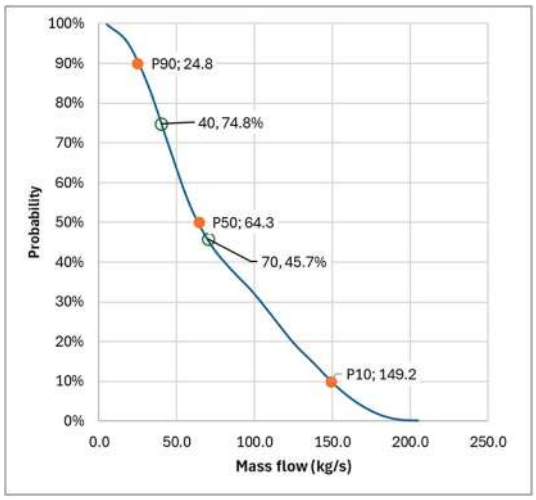

Fig. 17. Probability curve of the mass flow from a doublet. In orange are reported the corresponding values P10, P50, P90. The green circles are referred to the two values of mass flow from numerical simulation. (For interpretation of the references to colour in this figure legend, the reader is referred to the Web version of this article.)

trend after the 70's (Fig. 15b). 63 % of the buildings have been built after 1971, and the specific energy demand is lower than the average value of 102 kWh/m^2 per year.

The methodology used for evaluating the yearly energy demand of the building heritage is based on the data collected during the census in 2011 at scale of census section [88]. This allows us to select the possible area to be supplied by the district heating service. The selection criterion to identify the sections to be candidates for district heating service is the inhabitant density per kilometer. The selected areas correspond to the municipality, accounting for 66.1 % of the total heat demand (green area in Fig. 16). Some areas were added to the criterion of contiguity. Based on the number of heating hours, the power to satisfy this energy requirement is 10.7 MW.

The reservoir simulation indicates the possibility of producing up to 70 kg/s for more than 30 years without interaction with the injector.

The design of a District Heating plant is proposed to supply the Grottaminarda municipality. The well productivity is evaluated with the software DoubleCalc 1.4.3 [89] developed by TNO. The simulation, using as input data the results from the reservoir model, allows us to obtain the probability curve for the mass flow produced by the well (Fig. 17). Based on the numerical model, two main scenarios are chosen at 40 and 70 kg/s. The probability of success for those scenarios is between 75 % and 46 % respectively.

In the present application, for both scenarios the reinjection temperature is fixed to 65 °C. The pump pressure difference is fixed at 35 bar and the pump is located at 100 m depth. These assumptions ensure the reinjection avoiding possible CO_2 degassing from the brine.

Referring to scenario A with a mass rate of 40 kg/s, the wellhead temperature obtained is 134.5 °C, from 139 °C at 2600 m, and it requires a pumping system with 186 kW electrical power for a 35 bar of pump head. This requirement dramatically impacts on the operational costs. Therefore, a small Organic Rankine Cycle (ORC) unit with a power of 84 kW is installed to partially supply the request of electrical energy for well pumping (Fig. 18, Table 6). The electrical network will supply the circulation pump with 5 kW power.

Scenario B, with a production mass flow of 70 kg/s, shows a wellhead temperature of 136 °C. The scheme of the plant is identical to the previous one and the ORC plant has an electrical power of 863 kW (Fig. 18), while the well requires a pump power of 327 kW (Table 6).

A life cycle cost assessment (LCCA) was conducted to compare the two scenarios. The economic assumptions, NPV, annual interest rate,

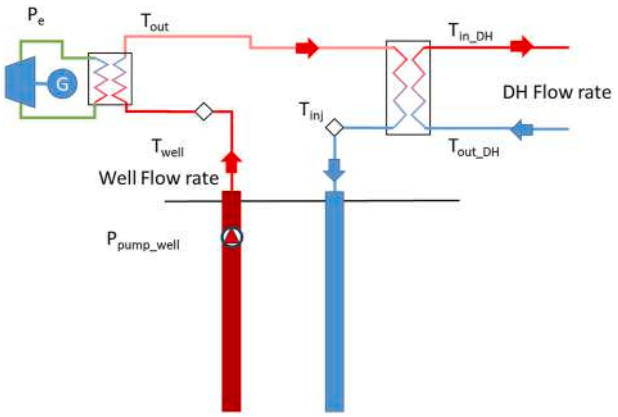

Fig. 18. Exploitation scheme. District Heating plant including the ORC for electrical power generation.

and the effects of the unit sales cost of heat and electricity on the economic parameters, such as the levelized cost of heat produced, payback period, IRR, and annual payback cost, were examined over the economic life of the system (Table 7). The evaluation of the costs was realized by applying the methodology presented by Alimonti et al. [88]. The economic analysis was conducted assuming a long-term lifetime of 30 years, and the annual operating hours were 8000 h, generally used in geothermal plants. The annual interest rate is obtained by combining the effective discount rate (4.25 %) and the annual average inflation rate (5.3 %) in August 2023.

A key element is the heat tariff. Realistic values were obtained from the survey conducted by the Italian regulatory authority for energy networks and environment (Autorità di Regolazione per Energia Reti e Ambiente, ARERA) in 2022 [90]. Before the energy crisis in 2022, the average price was 100.5 €/MWh, which will be used in the LCCA. The electrical energy prices are 0,16 €/kWh to buy and 0,08 €/kWh to sell.

The economics of scenario A with 40 kg/s are inconsistent with a negative NPV. The main issue is the cost for electrical energy accounting for 60 M€ that makes the Operational costs too high.

In scenario B with mass flow of 70 kg/s the economics largely differs. The larger ORC plant allows us to cover the electrical energy supply either for well pump, or for district heating distribution pump. The economic indexes highlight a positive Net Present Value (NPV) equal to 5.3 M€, a PBP of 6.3 years and an IRR of 15 %. The Levelized Cost of Heat (LCOH) is 98.1 €/MWh which is lower than the adopted tariff of 100.5 €/MWh. The impact of electrical energy production has an important role in reducing the OPEX to 0.4 M€. The LCOE is 0.33 €/kWh and remains higher than the average for geothermal plants, which is equal to 0.07 €/kWh, but the larger contribution is to make the project rentable. The CAPEX has increased to 16.6 M€ considering the larger binary plant. The income is given not only from the heat sales but also from the electrical energy sales. Finally, the scenario with a mass flow of 70 kg/s appears to be economically favorable and the probability of success is 46 % suggesting a good opportunity to realize the plant.

Table 6
Summary of the main parameters of the two scenarios. The variables are referred to Fig. 18.

Scenario	A	B
Well Flow rate (kg/s)	40	70
T_{well} (°C)	134.5	136
P_{pump_well} (kW)	186	327
T_{out} (°C)	128.6	101.4
P_e (kWe)	84	863
T_{inj} (°C)	65	65
T_{in_DH} (°C)	90	90
T_{out_DH} (°C)	60	60
DH Flow rate (kg/s)	84.8	84.8

Table 7
Life cycle cost assessment – Investment and operational costs of the project and economical results indexes. Operational costs are on an annual basis.

Scenario	A (M€)	B (M€)
INVESTMENT COSTS		
Drilling of 2 wells at 3000 m	11.12	11.12
Pipelines – main lines	1.5	1.5
Surface equipment	2.5	3.5
Surveys, Studies and design	0.33	0.33
OPERATIONAL COST		
Electrical energy for DH pump	1.55	–
Electrical energy for Well pump	59.49	–
Operation and Maintenance	0.37	0.37
ECONOMIC RESULTS		
LCOH (€MWh)	2973.2	98.1
LCOE (€/kWh)	217.35	0.33
NPV (M€)	−585.8	5.3
PBP (year)	7.63	6.2
IRR	11 %	15 %

7. Discussion and conclusions

The pressing need of reducing CO_2 emissions and achieving the carbon neutrality by 2050, as ratified at the COP 26 [1], requires the adoption of urgent measures. In recent decades, various scientific studies [10–14] proved that the use of geothermal energy for heating and cooling purposes can contribute to the CO_2 emission reduction, as well as to the reduction of energy supply costs and a long-term economic growth. However, this energy source is currently underutilized due to the high capital expenditures (CAPEX) for the exploration phase and well drilling [13] and for the associated mining risks. The use of pre-existing subsurface data derived from previous O&G exploration activities can contribute to the reduction of the exploration costs and of the mining risks, increasing the economic sustainability of geothermal projects. Noticeably, the development of geothermal resources has been successfully promoted by the availability of online databases of seismic data and well information [91], gathered by past oil and gas operators, even in countries in different geological settings, such as Germany [13], Netherland [14], Denmark [92] or Croatia [93].

In this contribution we propose a geothermal feasibility study of the Guardia Lombardi area, located in Southern Italy (Fig. 1), from the evaluation of the geothermal potential and its exploitation, carried out using vintage O&G subsurface data, up to the design of a heating/cooling and electricity production system. The cost-benefit evaluation of the geothermal project is also presented. Notwithstanding some limitations in the data quality discussed in the data and methodology section, our case study demonstrates that the availability of pre-existing O&G datasets saves all the costs related to the exploration phases. As an example, the about 700 km of already available 2D seismic profiles in the Guardia Lombardi area may correspond to a new acquisition cost of at least 7 M€ [94].The analysis of the well data revealed the presence of two main stratigraphic intervals in the study area subsurface, from bottom to top: fractured carbonate rocks (Cretaceous-Eocene time), belonging to the Apulian Carbonate Platform, and marly-clayey formations, belonging to the allochthonous and Pliocene units (Fig. 4). These lithological intervals are characterized by different porosity and permeability values; the allochthonous units are characterized by very low permeability values, while the carbonate units are characterized by the presence of some fractured intervals with high porosity and permeability values (e.g., up to 100–135 mD in Bonito 1 Dir well and 80–160 mD in Monte Forcuso 1 well; see Figs. 6 and 7 and Table 3). The SBHTs extrapolated for the deep wells reveal a significant geothermal anomaly in the study area, with a maximum temperature value of about 125 °C at just 2300 m depth in Bonito 1 Dir well (Fig. 5).

As highlighted by the seismic dataset interpretation and the 3D

geological modeling, a wide anticline affecting the Apulian Platform carbonates buried below the marly-clayey allochthonous and Pliocene units is located in the study area subsurface. This structure is characterized by two main culminations: Monte Forcuso and Bonito culminations (Fig. 10a). The highest and wider Monte Forcuso culmination is occupied by a CO_2 gas cap which is up to 470–500 m thick in the culmination area. Below, a CO_2-brackish water transition was intercepted. The CO_2 emission at the Mefite d'Ansanto hydrothermal spring is likely originated by the interaction between high-angle normal faults (i.e., the Mefite D'Ansanto Fault System) and the CO_2 gas cap. On the contrary, given the deeper position of the carbonate top, the surrounding deep wells (i.e., Bonito 1 Dir, Ciccone 1 and Monte Forcuso 2) just intercept the underlying brackish water deep aquifer, that occupies the smaller Bonito culmination (See Fig. 10b).

The review of the hydraulic tests revealed a hydrostatic pressure condition in the deep aquifer hosted in the fractured carbonate rocks in all the wells, but not in the Monte Forcuso 1 well that shows an overpressure due to the non-compensated CO_2 gas cap.

The structural and stratigraphic setting reconstruction and the analysis of the main rock properties suggest the existence of a geothermal reservoir in the Guardia Lombardi area subsurface. The anticline geometry, the high porosity and permeability values, the high temperatures and the presence of a suitable aquifer, make the Apulian Platform carbonates excellent reservoir rocks, while the marly-clayey lithology and the low permeability values make the overlying allochthonous and Pliocene units effective cap rocks (Figs. 4 and 10b).

As stated by Bayer et al. [12], the exploitation results of the geothermal resources depend on the geothermal system characteristics and the method used. In this case study, the availability of a large amount of pre-existing subsurface seismic reflection and well data allowed to properly characterize the geothermal system, while the numerical simulation results establish the best cultivation scheme (i.e., doublet scheme) and the more appropriate production value as to guarantee the exploitation of the detected geothermal resource. To ensure an advantage for the local community a heating/cooling plant was chosen, and the best economic conditions define the more appropriate scenario.

Future research direction can be identified in the integration of different data sources with advanced AI algorithms, forward modelling methods (stratigraphic or fracture network), the use of classical models in enhancing understanding and quantifying uncertainty. For example, the GO-FORWARD project [95] tests such approaches in areas with abundant subsurface information and production data, to prove conceptually the applicability of the methods and reproducibility of the results, to optimize and de-risk geothermal exploration in the same way of this work. The digitalization is another possible future application of the existing databases and can help in building digital twins for geothermal energy production and underground heat storage systems.

The potential environmental impacts and safety protocols associated with the development of geothermal resources has been recently evaluated in several studies, even with a special focus on Italy [96,97]. These studies demonstrate that the current safety protocols can effectively mitigate the potential negative implications associated with geothermal drilling and fluid reinjection.

Given the above, the methodology adopted in this case study, based on the use of pre-existing O&G data, has proven effective in producing significant economic benefits due to the reduction of the geothermal exploration costs. Moreover, the mining risks of the geothermal exploration phase are eliminated or significantly reduced. For these reasons, we believe that a reassessment of the geothermal potential of already explored hydrocarbon basins, widespread around the world, could encourage the use of geothermal energy and contribute to the achievement of the carbon neutrality goals, resulting in environmental, economic and social benefits.

CRediT authorship contribution statement

Michele Livani: Writing – original draft, Validation, Methodology, Formal analysis, Data curation. **Barbara Inversi:** Writing – review & editing, Validation, Methodology, Formal analysis, Data curation, Conceptualization. **Giordano Montegrossi:** Writing – original draft, Validation, Methodology, Formal analysis, Data curation, Conceptualization. **Lorenzo Petracchini:** Writing – review & editing, Validation, Methodology, Formal analysis, Data curation. **Claudio Alimonti:** Writing – original draft, Methodology, Formal analysis, Conceptualization. **Davide Scrocca:** Writing – review & editing, Supervision, Project administration, Methodology, Funding acquisition, Formal analysis, Conceptualization.

Funding sources

Part of this work was supported by the VIGOR Project, whose activities are part of the Italian Interregional Program "Renewable Energies and Energy Savings FESR 2007–2013 – Axes I Activity line 1.4 "Experimental Actions in Geothermal Energy".

Declaration of competing interest

The authors declare that they have no known competing financial interests or personal relationships that could have appeared to influence the work reported in this paper.

Acknowledgments

Part of this study has been originally carried out in the frame of the VIGOR Project, aimed at assessing the geothermal potential and exploring geothermal resources of four regions in southern Italy. The authors wish to thank all the colleagues of the Vigor Project working group, and particularly the Project coordinator Adele Manzella, for fruitful discussions. We also thank ENI S.p.A. for making available, under a confidential agreement, the seismic reflection profiles and well data used in this work. Special thanks to Alessandro Romi for his appreciated support with Petrel® Software (Schlumberger).

Appendix A. Supplementary data

Supplementary data to this article can be found online at https://doi.org/10.1016/j.renene.2025.122401.

References

[1] COP-26, Report of the conference of the Parties on its twenty-sixth session, held in glasgow from 31 october to 13 november 2021, decisions adopted by the conference of the Parties, 1/CP.26 glasgow, Climate Pact (2021). https://unfccc.int/documents/460954. (Accessed 16 December 2024).
[2] H. Lee, J. Romero, Climate Change 2023: Synthesis Report. Contribution of Working Groups I, II and III to the Sixth Assessment Report of the Intergovernmental Panel on Climate Change, IPCC, Geneva, Switzerland, 2023, https://doi.org/10.59327/IPCC/AR6-9789291691647.
[3] United Nations Environment Programme, Emissions gap report 2022. https://www.unep.org/emissions-gap-report-2022, 2022. (Accessed 4 July 2024).
[4] G. McGranahan, D. Balk, B. Anderson, The rising tide: assessing the risks of climate change and human settlements in low elevation coastal zones, Environ. Urban. 19 (2007) 17–37, https://doi.org/10.1177/0956247807076960.
[5] G.B. Bonan, Forests and climate change: forcings, feedbacks, and the climate benefits of forests, Science 320 (2008) 1444–1449, https://doi.org/10.1126/science.1155121.
[6] M.A. Bender, T.R. Knutson, R.E. Tuleya, J.J. Sirutis, G.A. Vecchi, S.T. Garner, I. M. Held, Modeled impact of anthropogenic warming on the frequency of intense atlantic hurricanes, Science 327 (5964) (2010) 454–458, https://doi.org/10.1126/science.1180568.
[7] J. Hansen, R. Ruedy, M. Sat, K. Lo, Global surface temperature change, Rev. Geophys. 48 (2010) RG4004, https://doi.org/10.1029/2010RG000345.
[8] R.A. Anthes, R.W. Corell, G. Holland, J.W. Hurrell, M.C. MacCracken, K. Trenberth, Hurricanes and global warming—potential linkages and consequences, BAMS 87 (2006) 623–628, https://doi.org/10.1175/BAMS-87-5-617.

[9] A. Cazenave, How fast are the ice sheets melting? Science 314 (2006) 1251–1252, https://doi.org/10.1126/science.1133325.

[10] European technology and innovation platform on geothermal (ETIP-G), geothermal horizons: from cities to regions. https://www.egec.org/media-publications/geothermal-horizons-from-cities-to-regions-is-now-live/, 2024. (Accessed 16 December 2024).

[11] M. Soltani, F. Moradi Kashkooli, M. Souri, B. Rafiei, M. Jabarifar, K. Gharali, J. S. Nathwani, Environmental, economic, and social impacts of geothermal energy systems, Renew. Sustain. Energy Rev. 140 (2021) 110750, https://doi.org/10.1016/j.rser.2021.110750.

[12] P. Bayer, G. Attard, P. Blum, K. Menberg, The geothermal potential of cities, Renew. Sustain. Energy Rev. 106 (2019) 17–30, https://doi.org/10.1016/j.rser.2019.02.019.

[13] T. Agemar, J. Alten, B. Ganz, J. Kuder, K. Kühne, S. Schumacher, R. Schulz, The geothermal information system for Germany, GeotIS - ZDGG 165 (2014) 129–144.

[14] M.A.W. Vrijlandt, E.L.M. Struijk, L.G. Brunner, J.G. Veldkamp, N. Witmans, D. Maljers, J.D. Van Wees, ThermoGIS: from a static to a dynamic approach for national geothermal resource information and development. Proceedings World Geothermal Congress 2020, Reykjavik, Iceland, 26 .

[15] B. Della Vedova, I. Bottio, M. Cei, P. Conti, G. Giudetti, G. Gola, L. Spadoni, M. Vaccaro, L. Xodo, Geothermal energy use, country update for Italy, Proceedings European Geothermal Congress (2022). Berlin, Germany, 17-21 October 2022.

[16] ENEL Gren Power, L'energia geotermica in Italia: dove viene prodotta e come. https://www.enelgreenpower.com/it/learning-hub/energie-rinnovabili/energia-geotermica/italia. (Accessed 25 June 2024).

[17] F. Mostardini, S. Merlini, Appennino centro-meridionale, Sezioni geologiche e proposta di modello strutturale, Mem, Soc. Geol. It. 35 (1986) 177–202.

[18] C. Turrini, P. Rennison, Structural style from the Southern Apennines' hydrocarbon province - an integrated view, in: K.R. McClay (Ed.), Thrust Tectonics and Hydrocarbon Systems, vol. 82, AAPG Memoir, 2004, pp. 558–578.

[19] C. Nicolai, R. Gambini, Structural architecture of the Adria platform-and-basin system, in: A. Mazzotti, E. Patacca, P. Scandone (Eds.), Results of the CROP Project Sub-project CROP-04 Southern Apennines (Italy), vol. 7, 2007, pp. 21–37. Boll. Soc. Geol. It. (Italian Journal of Geoscience) special issue.

[20] E. Patacca, P. Scandone, Geology of the southern Apennines, in: A. Mazzotti, E. Patacca, P. Scandone (Eds.), Results of the CROP Project Sub-project CROP-04 Southern Apennines (Italy), vol. 7, 2007, pp. 75–119. Boll. Soc. Geol. It. (Italian Journal of Geoscience) special issue.

[21] F. Bertello, R. Fantoni, R. Franciosi, V. Gatti, M. Ghielmi, A. Pugliese, From thrust-and-fold belt to foreland: hydrocarbon occurrences in Italy, in: petroleum geology: from mature basins to new frontiers, in: Proceedings of the 7th Petroleum Geology Conference, Geological Society of, London, London, 2010, pp. 113–126, https://doi.org/10.1144/0070113.

[22] B. Inversi, D. Scrocca, G. Montegrossi, M. Livani, L. Petracchini, M. Brandano, M. Brilli, F. Giustini, R. Recanati, G. Gola, M. Polemio, A. Romi, R. de Franco, G. Caielli, B. Testa, 3D geological modelling of a fractured carbonate reservoir for the study of medium enthalpy geothermal resource in Southern Apennines (Campania Region, Italy), Extended abstract European Geothermal Congress, Pisa, Italy (June 2013) 3–7.

[23] C. Albanese, A. Allansdottir, L. Amato, F. Ardizzone, S. Bellani, G. Bertini, S. Botteghi, D. Bruno, G. Caielli, F. Caiozzi, A. Caputi, R. Catalano, S. Chiesa, A. Contino, S. D'arpa, G. De Alteriis, R. de Franco, D. Dello Buono, E. Destro, E. Di Sipio, A. Donato, M. Doveri, V. Dragone, A. Ellero, M. Fedi, L. Ferranti, G. Florio, M. Folino, A. Galgaro, C. Gennaro, G. Gianelli, A. Giaretta, G. Gola, G. Greco, P. Iaquinta, B. Inversi, M. Iorio, G. Iovine, F. Izzi, M. La Manna, M. Livani, G. Lombardo, N. Lopez, D. Magnelli, D. Maio, A. Manzella, I. Marchesini, G. Martini, G. Masetti, A. Mercadante, A. Minissale, D. Montanari, G. Montegrossi, S. Monteleone, F. Muto, G. Muttoni, G. Norini, A. Pellizzone, P. Perotta, L. Petracchini, S. Pierini, M. Polemio, E. Rizzo, L. Russo, M. Sabatino, F. Santaloia, A. Santilano, D. Scrocca, S. Soleri, C. Tansi, O. Terranova, G. Teza, G. Tranchida, E. Trumpy, V. Uricchio, V. Valenti, VIGOR: Sviluppo geotermico nelle Regioni della Convergenza, Rapporto tecnico prodotto nell'ambito del Progetto Vigor "Valutazione del potenziale geotermico delle regioni della convergenza" (POI Energie Rinnovabili e Risparmio Energetico, FESR 2007-2013), Editore CNR-IGG, Pisa (Italia), 2014, p. 161. ISBN 9788879580113, www.vigor-geotermia.it/images/download/volumi/VIGOR-Sviluppo-geotermico-regioni-convergenza.pdf.

[24] A. Amoresano, A. Angelino, M. Anselmi, B. Bianchi, S. Botteghi, M. Brandano, M. Brilli, P.P. Bruno, G. Caielli, A. Caputi, N. Cardellicchio, A. Carotenuto, G. Cavuoto, C. Chiarabba, S. Chiesa, M. Ciccolella, A. Corniello, E. Cuoco, B. de Fenzo, R. de Franco, G. De Lisa, G. De Luca, U. del Vecchio, G. Di Bella, V. di Fiore, C. di Gregorio, M. Di Leo, A. Donato, A. D'Oriano, D. Ducci, M. Fedi, L. Ferrante, G. Florio, V. Gargiulo, A. Gimelli, A. Giocoli, F. Giustini, G. Gola, M. Iavarone, B. Inversi, M. Iorio, G. Langella, M. Livani, S. Losanno, A. Manzella, S. Maraio, N. Massarotti, A. Mauro, S. Meo, A. Mercadante, A. Minissale, D. Montanari, G. Montegrossi, M. Mussi, L. Pandolfi, N. Pelosi, L. Petracchini, E. Petruccione, M. Pischiutta, M. Polemio, M. Punzo, F. Quattrocchi, R. Recanati, E. Rizzo, C. Romano, A. Romi, A. Rovelli, G. Sarnacchiaro, P. Scotto di Vettimo, D. Scrocca, S. Tamburrino, D. Tarallo, D. Tedesco, B. Testa, P. Tiano, L. Vanoli, F. Varriale, VIGOR: Sviluppo geotermico nella regione Campania - Studi di Fattibilità a Mondragone e Guardia Lombardi. Progetto VIGOR - Valutazione del Potenziale Geotermico delle Regioni della Convergenza, POI Energie Rinnovabili e Risparmio Energetico 2007-2013, CNR-IGG (2015). ISBN: 9788879580151, www.vigor-geotermia.it/images/download/fatt_volumi/CAMPANIA/Campania.pdf.

[25] A. Ebigbo, J. Niederau, G. Marquart, B. Inversi, D. Scrocca, G. Gola, J. Arnold, G. Montegrossi, C. Vogt, R. Pechnig, Evaluation of the Geothermal Energy Potential in the Medium-Enthalpy Reservoir Guardia dei Lombardi, Italy. Proceedings of the 39th Workshop on Geothermal Reservoir Engineering, Stanford University, Stanford, 2014. SGP-TR-202.

[26] J. Niederau, A. Ebigbo, G. Marquart, S.G. Mendoza, B. Inversi, G. Gola, D. Scrocca, A. Manzella, G. Montegrossi, C. Clauser, Assessment and simulation of various utilization scenarios of a medium-enthalpy reservoir in Southern Italy (Guardia Lombardi). Proceedings World Geothermal Congress 2015, Melbourne, 2015.

[27] B. Della Vedova, S. Bellani, G. Pellis, P. Squarci, Deep temperatures and surface heat flow distribution, in: G.B. Vai, I.P. Martini (Eds.), Anatomy of an Orogen: the Apennines and Adjacent Mediterranean Basins, Kluwer, Dordrecht, 2001, pp. 65–76, https://doi.org/10.1007/978-94-015-9829-3_7.

[28] ENEL, Inventario delle risorse geotermiche nazionali: regione Campania. https://unmig.mase.gov.it/inventario-delle-risorse-geotermiche-nazionali-rapporti-regionali/, 1987.

[29] ENEL/ENI/CNR/ENEA, Inventario delle risorse geotermiche nazionali, Valutazione del potenziale geotermico nazionale, Aggiornamenti 1994. https://unmig.mase.gov.it/inventario-delle-risorse-geotermiche-nazionali-aggiornamenti/, 1994.

[30] P. Budetta, P. Celico, A. Corniello, R. De Riso, D. Ducci, P. Nicotera, Carta idrogeologica del F. 186 (S. Angelo dei Lombardi), memoria illustrativa, Mem, Soc. Geol. It. 41 (1988) 1029–1038.

[31] B. Galdi, La Valle di Ansanto nella legenda e nella storia e il petrolio di Frigento, vol. 3, 1931, p. 24. Memorie Accad. Sci. Torino, Lettere ed Arti in Modena.

[32] F. Ortolani, M. De Gennaro, M. Ferreri, M.R. Ghiara, D. Stanzione, F. Zenone, Prospettive geotermiche dell'Irpinia centrale (Appennino meridionale): studio geologico-strutturale e geochimico, Boll. Soc. Geol. It. 100 (1981) 139–159.

[33] G. Chiodini, F. Frondini, F. Ponzani, Deep structures and carbon dioxide degassing in Central Italy, Geothermics 24 (1995) 81–94.

[34] S. Di Nocera, M. Imperato, F. Matano, D. Stanzione, G.M. Valentino, Caratteri geologici e idrogeochimici della Valle di Ansanto (Irpinia Centrale, Appennino Campano-Lucano), Boll. Soc. Geol. It. 118 (1999) 395–406.

[35] V. Duchi, A. Minissale, O. Vaselli, M. Ancillotti, Hydrogeochemestry of the Campania region in southern Italy, J. Volcanol. Geotherm. Res. 67 (1995) 313–328, https://doi.org/10.1016/0377-0273(94)00109-T.

[36] E. Carminati, C. Doglioni, D. Scrocca, Alps vs. Apennines, in: Special Volume of the Italian Geological Society for the 32nd International Geological Congress, Florence, Italy, 2004, pp. 141–151.

[37] E. Patacca, R. Sartori, P. Scandone, Tyrrhenian basin and Appeninic Arcs: kinematic relations since late Tortonian times, Mem. Soc. Geol. It. 45 (1990) 425–451.

[38] L. Royden, E. Patacca, P. Scandone, Segmentation and configuration of subducted lithosphere in Italy: an important control on thrust-belt and foredeep-basin evolution, Geology 15 (1987) 714–717.

[39] C. Doglioni, A proposal for the kinematic modelling of W-dipping subductions; possible applications to the Tyrrhenian-Apennines system, Terra. Nova 3 (1991) 423–434.

[40] A. Malinverno, W.B.F. Ryan, Extension in the Tyrrhenian Sea and shortening in the Apennines as result of arc migration driven by sinking of the lithosphere, Tectonics 5 (1986) 227–245.

[41] B. D'argenio, T. Pescatore, P. Scandone, Structural pattern of the campania-lucania Apennines, Quad. La Ric. Sci. 90 (1975) 313–327.

[42] P. Casero, F. Roure, L. Endignoux, I. Moretti, C. Muller, L. Sage, R. Vially, Neogene geodynamic evolution of the southern Apennines, Mem. Soc. Geol. It. 41 (1988) 109–120.

[43] I. Sgrosso, Nuovi dati biostratigrafici sul Miocene del Monte Alpi (Lucania) e conseguenti ipotesi paleogeografiche, Mem. Soc. Geol. It. 41 (1988) 343–351.

[44] E. Patacca, P. Scandone, M. Bellatalla, N. Perilli, U. Santini, The numidian-sand event in the southern Apennines, mem, Sci. Geol. 43 (1992) 297–337.

[45] E. Marsella, A.W. Bally, G. Cippitelli, B. D'argenio, G. Pappone, Tectonic history of the Lagonegro domain and Southern Apennine thrust belt evolution, Tectonophysics 252 (1995) 307–330, https://doi.org/10.1016/0040-1951(95)00097-6.

[46] A. Menardi Noguera, G. Rea, Deep structure of the campanian-lucanian arc (southern Apennines), Tectonophysics 324 (2000) 239–265, https://doi.org/10.1016/S0040-1951(00)00137-2.

[47] D. Scrocca, Southern Apennines: structural setting and tectonic evolution, J. Virtual Explor. 36 (2010), https://doi.org/10.3809/jvirtex.2010.00225 paper 14.

[48] L. Ogniben, Schema Introduttivo alla geologia del confine calabro-lucano, Mem. Soc. Geol. It. 8 (1969) 453–763.

[49] G. Bonardi, F.O. Amore, G. Ciampo, P. De Capoa, P. Miconnet, V. Perrone, Il Complesso Liguride auct.: stato delle conoscenze e problemi aperti sulla sua evoluzione pre-appenninica ed i suoi rapporti con l'Arco Calabro, Mem. Soc. Geol. It. 41 (1988) 17–35.

[50] G. Bonardi, B. D'Argenio, V. Perrone, Carta geologica dell'Appennino meridionale, Mem, Soc. Geol. It. 41 (1988). Table attached, 1: 500,000 scale.

[51] S. Vitale, S. Ciarcia, L. Fedele, F.D.A. Tramparulo, The Ligurian oceanic successions in southern Italy: the key to decrypting the first orogenic stages of the southern Apennines-Calabria chain system, Tectonophysics 750 (2019) 243–261, https://doi.org/10.1016/j.tecto.2018.11.010.

[52] S. Sartoni, U. Crescenti, Ricerche biostratigrafiche nel Mesozoico dell'Appennino meridionale, Giorn, Geol. 29 (1961) 161–302.

[53] R. Selli, Sulla trasgressione del Miocene nell'Italia meridionale, Giorn, Geol. 26 (1957) 1–54.

[54] R. Selli, Il Paleogene nel quadro della geologia dell'Italia meridionale, Mem, Soc. Geol. It. 3 (1962) 733–789.

[55] P. Scandone, Studi di geologia lucana: la serie calcareo-silico-marnosa e i suoi rapporti con l'Appennino Calcareo, Boll. Soc. Nat. Napoli 76 (1967) 301–469.

[56] P. Scandone, Studi di geologia lucana: la carta dei terreni della serie calcareo-silico-marnosa e note illustrative, Boll. Soc. Nat. Napoli 81 (1972) 225–300.
[57] S. Carbone, S. Catalano, F. Lentini, C. Monaco, Le unita' stratigrafico-strutturali dell'Alta Val d'Agri (Appennino Lucano) nel quadro dell'evoluzione del sistema catena-avanfossa, Mem, Soc. Geol. It. 41 (1988) 331–341.
[58] S. Carbone, F. Lentini, Migrazione neogenica del sistema catena-avampaese nell'Appennino meridionale: problematiche paleogeografiche e strutturali, Riv. Ital. Paleontol. Stratigr. 96 (1990) 271–296.
[59] D. Scrocca, S. Sciamanna, E. Di Luzio, M. Tozzi, C. Nicolai, R. Gambini, Structural setting along the CROP-04 deep seismic profile (Southern Apennines - Italy), in: A. Mazzotti, E. Patacca, P. Scandone (Eds.), Results of the CROP Project Sub-project CROP-04 Southern Apennines (Italy), vol. 7, 2007, pp. 283–296. Boll. Soc. Geol. It. (Italian Journal of Geoscience) special issue.
[60] G. Ricchetti, N. Ciaranfi, E. Luperto Sinni, F. Monelli, P. Pieri, Geodinamica ed evoluzione sedimentaria e tettonica dell'avampaese apulo, Mem, Soc. Geol. It. 41 (1988) 57–82.
[61] G. Ciarapica, L. Passeri, The paleogeographic duplicity of the Apennines, Boll. Soc. Geol. It. special 1 (2002) 67–75.
[62] G.M. Stampfli, G.D. Borel, R. Marchant, J. Mosar, Western Alps geological constraints on western Tethyan reconstructions, in: G. Rosenbaum, G.S. Lister (Eds.), Reconstruction of the Evolution of the Alpine-Himalayan Orogen, vol. 7, Journal of the Virtual Explorer, 2002, pp. 75–104, https://doi.org/10.3809/jvirtex.2002.00057.
[63] E. Patacca, P. Scandone, Late thrust propagation and sedimentary response in the thrust belt-foredeep system of the Southern Apennines, in: G.B. Vai, I. P Martini (Eds.), Anatomy of an Orogen: the Apennines and Adjacent Mediterranean Basin, Kuwler Academic Publishers, Dordrecht, 2001, pp. 401–440.
[64] G. Cello, S. Mazzoli, Apennine tectonics in southern Italy: a review, J. Geodyn. 27 (1999) 191–211, https://doi.org/10.1016/S0264-3707(97)00072-0.
[65] F. Brozzetti, The Campania-Lucania Extensional Fault System, southern Italy: a suggestion for a uniform model of active extension in the Italian Apennines, Tectonics 30 (2011) TC5009, https://doi.org/10.1029/2010TC002794.
[66] S. Catalano, C. Monaco, L. Tortorici, W. Paltrinieri, N. Steel, Neogene-Quaternary tectonic evolution of the southern Apennines, Tectonics 23 (2004) TC2003, https://doi.org/10.1029/2003TC001512.
[67] L. Ferranti, F. carboni, A. Akimbekova, M. Ercoli, S. Bello, F. Brozzetti, A. Bacchiani, G. Toscani, Structural architecture and tectonic evolution of the Campania-Lucania arc (Southern Apennines, Italy): constraints from seismic reflection profiles, well data and structural-geologic analysis, Tectonophysics 230313 (2024), https://doi.org/10.1016/j.tecto.2024.230313.
[68] F. Feriozzi, L. Improta, F.E. Maesano, P. De Gori, R. Basili, The 3D crustal structure in the epicentral region of the 1980, Mw 6.9, Southern Apennines earthquake (southern Italy): New constraints from the integration of seismic exploration data, deep wells, and local earthquake tomography, Tectonics 43 (2024) e2023TC008056, https://doi.org/10.1029/2023TC008056.
[69] S. Mazzoli, S. Corrado, M. De Donatis, D. Scrocca, R.W.H. Butler, D. Di Bucci, G. Naso, C. Nicolai, V. Zucconi, Time and space variability of "thin-skinned'' and "thick-skinned'' thrust tectonics in the Apennines (Italy), Rend, Lincei Sci. Fis. Nat. 11 (2000) 5–39.
[70] R.W.H. Butler, S. Mazzoli, S. Corrado, M. De Donatis, D. Di Bucci, R. Gambini, G. Naso, C. Nicolai, D. Scrocca, P. Shiner, V. Zucconi, Applying thick-skinned tectonic models to the Apennine thrust belt of Italy - limitations and implications, in: K.R. McClay (Ed.), Thrust Tectonics and Hydrocarbon Systems, vol. 82, AAPG Memoir, 2004, pp. 647–667, https://doi.org/10.1306/M82813C34.
[71] D. Scrocca, E. Carminati, C. Doglioni, Deep structure of the southern Apennines, Italy: thin-skinned or thick-skinned? Tectonics 24 (2005) TC3005 https://doi.org/10.1029/2004TC001634.
[72] S. Tavani, P. Granado, A. Corradetti, G. Camanni, G. Vignaroli, G. Manatschal, S. Mazzoli, J.A. Muñoz, M. Parente, Rift inheritance controls the switch from thin- to thick-skinned thrusting and basal décollement re-localization at the subduction-to-collision transition, GSA Bulletin 133 (2021) 2157–2170, https://doi.org/10.1130/B35800.1.
[73] G. Bonardi, S. Ciarcia, S. Di Nocera, M. Matano, I. Sgrosso, M. Torre, Carta delle principali unità cinematiche dell'Appennino meridionale, Nota illustrativa, Boll. Soc. Geol. It. 128 (2009) 47–60.
[74] F. Matano, S. Di Nocera, Geologia del settore centrale dell'Irpinia (Appennino Meridionale): nuovi dati e interpretazioni, Boll. Soc. Geol. It. 120 (2001) 3–14.
[75] S. Di Nocera, F. Matano, T.S. Perscatore, F. Pinto, R. Quarantiello, M.R. Senatore, M. Torre, Schema geologico del transetto Monti Picentini orientali – Monti della Daunia meridionali: unità stratigrafiche ed evoluzione tettonica del settore esterno dell'Appennino meridionale, Boll. Soc. Geol. It. 125 (2006) 39–58.
[76] L. Vezzani, A. Festa, F.C. Ghisetti, Geology and tectonic evolution of the central-southern Apennines, Italy, GSA 469 (2010) 1–58, https://doi.org/10.1130/SPE469.
[77] VIDEPI Project, Visibility of petroleum exploration data in Italy, ministry for economic development DGRME - Italian geological society - assomineraria. https://www.videpi.com/videpi/videpi.asp.
[78] A. Förster, D.F. Merriam, J.C. Davis, Spatial analysis of temperature (BHT/DST) data and consequences for heat-flow determination in sedimentary basins, Geol. Rundsch. 86 (1997) 252–261.
[79] K. Pruess, C. Oldenburg, G. Moridis, TOUGH2 User's Guide, Version 2, Earth Sciences Division, Lawrence Berkeley National Laboratory, University of California, Berkeley, California, 2012. LBNL-43134.
[80] G. Chiodini, C. Cardellini, A. Amato, E. Boschi, S. Caliro, F. Frondini, G. Ventura, Carbon dioxide Earth degassing and seismogenesis in central and southern Italy, Geophys. Res. Lett. 31 (2004) L07615, https://doi.org/10.1029/2004GL019480.
[81] G. Chiodini, D. Granieri, R. Avino, S. Caliro, A. Costa, C. Minopoli, G. Vilardo, Non-volcanic CO_2 earth degassing: case of mefite d'Ansanto (southern Apennines), Italy, Geophys. Res. Lett. 37 (2010) L11303, https://doi.org/10.1029/2010GL042858.
[82] G. Montegrossi, B. Cantucci, O. Vaselli, F. Quattrocchi, Reconstruction of porosity profile in an off-shore well, Boll. Geofis. Teor. Appl. 49 (2008) 408–410.
[83] C.F. Williams, Updated methods for estimating recovery factors for geothermal resources. Proceedings of 32nd Workshop on Geothermal Reservoir Engineering, Stanford University, Stanford, 2007. SGP-TR-183.
[84] M.A. Grant, S.K. Garg, Recovery factor for EGS, in: Proceedings of the 37th Workshop on Geothermal Reservoir Engineering, Stanford University, Stanford, 2012. SGP-TR-194.
[85] EUROSTAT, SHort Assessment of Renewable Energy Sources, SHARES up to 2020 and 2021 summary results (2023). https://ec.europa.eu/eurostat/web/energy/database/additional-data#Short%20assessment%20of%20renewable%20energy%20sources%20(SHARES. (Accessed 4 July 2024).
[86] Weather Spark, Climate and average weather year round in Grottaminarda. https://weatherspark.com/y/78838/Average-Weather-in-Grottaminarda-Italy-Year-Round. (Accessed 4 July 2024).
[87] Gazzetta Ufficiale, Decreto del Presidente della Repubblica 26 agosto, 1993, p. 142. https://www.gazzettaufficiale.it/eli/id/1993/10/14/093G0451/sg. (Accessed 27 June 2024), 1993.
[88] C. Alimonti, F. Vitali, D. Scrocca, Reuse of oil wells in geothermal district heating networks: a sustainable opportunity for cities of the future, Energies 17 (2024) 169, https://doi.org/10.3390/en17010169.
[89] H.F. Mijnlieff, A.N.M. Obdam, J.D.A.M. van Wees, M.P.D. Pluymaekers, J. G. Veldkamp, DoubletCalc 1.4 manual - English version for DoubletCalc 1.4.3. https://www.nlog.nl/sites/default/files/6ab98fc3-1ca1-4bbe-b0a2-c5a9658a3597_doubletcalc%20v143%20manual.pdf, 2014. (Accessed 4 July 2024).
[90] ARERA, Relazione annuale. https://www.arera.it/chi-siamo/relazione-annuale/relazione-annuale-2022, 2022. (Accessed 5 July 2024), 2022.
[91] M. Brémaud, N.M. Burnside, Z.K. Shipton, C.J. Willems, De-risking database for hot sedimentary aquifers. Proceedings World Geothermal Congress 2023, 2023. Beijing, China.
[92] H. Vosgerau, A. Mathiesen, L.H. Nielsen, Facilitating the utilization of deep geothermal energy in Denmark by regional derisking using hydrocarbon data. Proceedings AAPG European Region, 3rd Hydrocarbon Geothermal Cross over Technology Workshop, 9-10 April 2019. Geneva, Switzerland.
[93] Croatian Hydrocarbon Agency, Invest in geothermal, Croatia, geothermal booklet. https://azu.hr/media/rqfjolpe/invest-in-geothermal-croatia1.pdf, 2023. (Accessed 3 December 2024).
[94] M. Ireland, C. Dunham, J. Gluyas, *Seismic for geothermal*. Geoscientist. https://geoscientist.online/sections/unearthed/seismic-for-geothermal/, 2023. (Accessed 16 December 2024).
[95] CORDIS, Geothermal exploration and optimization through forward modelling and resource development. https://cordis.europa.eu/project/id/101147618, 2024. (Accessed 12 December 2024).
[96] G.M. Idroes, I. Hardi, I.S. Hilal, R.T. Utami, T.R. Noviandy, R. Idroes, Economic growth and environmental impact: assessing the role of geothermal energy in developing and developed countries, Innovation and Green Development 3 (2024) 100144, https://doi.org/10.1016/j.igd.2024.100144.
[97] A. Manzella, R. Bonciani, A. Allansdottir, S. Botteghi, A. Donato, S. Giamberini, A. P.M. Lenzi, A. Pellizzone, D. Scrocca, Environmental and social aspects of geothermal energy in Italy, Geothermics 72 (2018) 232–248, https://doi.org/10.1016/j.geothermics.2017.11.015.